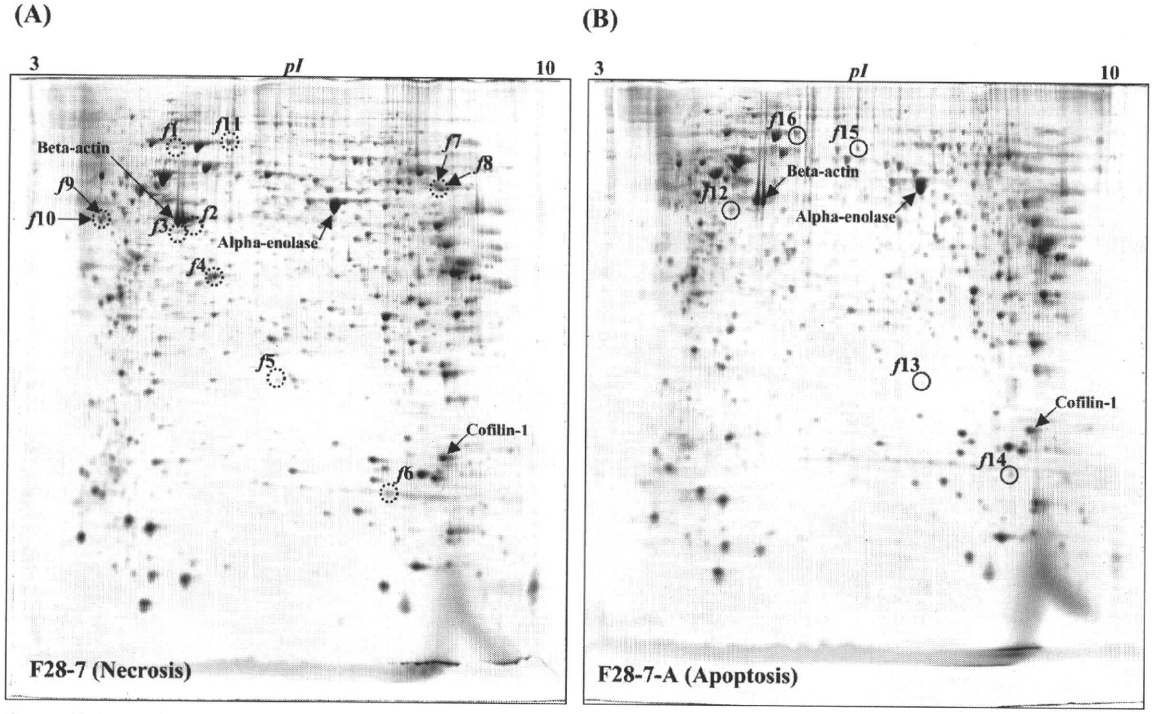

Figure 2. Sypro Ruby-stained 2D gels of FUdR-induced necrosis in F28-7 and apoptosis in F28-7-A cells. (A) Proteome 2D-map of F28-7 cells undergoing FUdR-induced necrosis (reproducibility confirmed; $n = 3$). (B) Proteome 2D-map of F28-7-A cells undergoing FUdR-induced apoptosis (reproducibility confirmed; $n = 3$). F28-7 and F28-7-A cells were treated with 1 μM FUdR for 16 h. Whole cell lysates were prepared and they were individually focused on a pH 3−10 nonlinear range IPG strip and then separated on a 12.5% SDS-PAGE gel, stained, and visualized as described under Materials and Methods. The spots *f*1−*f*11 displayed in the 2D-map of F28-7 cells (A) gave corresponding spots of lower intensities for F28-7-A (B). The spots *f*12−*f*16 displayed in the 2D proteome map of F28-7-A cells (B) gave spots of lower intensities for F28-7 (A). Protein spots are identified by MALDI-TOF MS, MALDI-TOF/TOF MS, and nano-LC−MS/MS.

of these identified proteins, their Swiss-prot database accession numbers, spot designation, reported isoelectric points and molecular weight values, along with associated biological processes (functions). In addition, data were obtained for the identification of the focused protein spots based on peptide mass fingerprint and MS/MS experiments (see Supplementary Tables 1 and 2, Supporting Information). The functions associated with these proteins include chromatin modification, cytoskeleton organization, signal transduction, glutathione metabolism, stress response, purine nucleotide biosynthesis, carnitine metabolism, redox homeostasis, and protein folding. These identified proteins are those functioning at various stages of important biological processes.

The accuracy of the proteome results was confirmed using traditional immunological techniques. Thus, we analyzed the expression levels of the identified proteins by Western blotting. The analysis showed that the relative levels of cytokeratin-19, cytokeratin-8, and annexin A1 in F28-7, in comparison to those in F28-7-A cells, were 33.3, 5.0, and 10.0, respectively (Supplementary Figure 1, Supporting Information). The high expressions of these proteins in Western blotting conform with the results of proteome analysis.

Protein Expression Analysis of FUdR-Induced Necrosis and Apoptosis. Next, we examined the effect of FUdR-treatment on the proteome profiles. F28-7 and F28-7-A cells were treated with 1 μM FUdR for 16 h. The treatment with FUdR caused induction of necrosis in F28-7 and apoptosis in F28-7-A cells.[5] We previously found that the release of cytochrome c from mitochondria into both the cytoplasm and the nucleus induced apoptosis but not necrosis.[6] This key phenomenon occurred at 16 h after treatment with FUdR. Therefore, we performed proteome analysis at the 16 h. Cell lysates were analyzed using 2-DE to detect changes in the necrosis and apoptosis cell-proteomes. Figure 2A and B shows typical two-dimensional gels of the necrosis and apoptosis cell-lysates. Approximately 1800 protein spots per gel were reproducibly detected. Using a 1.5-fold cutoff, the analysis identified 16 altered protein spots: 11 high intensity spots and 5 low intensity spots in necrosis (F28-7) compared to apoptosis cells (F28-7-A), which accounted for about 1% of the total number of detectable proteins. Twenty-four proteins were identified in these 16 spots by MS analysis using MALDI-TOF MS, MALDI-TOF/TOF MS, and nano-LC−MS/MS. The expression levels of the 24 proteins were significantly different between the necrosis and apoptosis cells. Among them, 13 proteins were consistently higher and 11 proteins were consistently lower in abundance in the necrosis cells. Table 2 lists the names and features of the 24 proteins. In addition, a complete list of data is available for the identification of the focused protein spots based on peptide mass fingerprints and MS/MS experiments (see Supplementary Tables 1 and 3, Supporting Information). The protein functions thus found to differ between necrosis and apoptosis were chromatin modification, cytoskeleton organization, glycolysis, ATP biosynthesis, glycine metabolism, protein folding, and galactose metabolism. Remarkably, a number of the mitochondrial proteins exhibited the differential expressions. These proteins include pyruvate dehydrogenase E1 component subunit beta, ATP synthase subunit alpha, stress-70 protein (GRP75), peptidyl-tRNA hydrolase 2, and pyruvate kinase isozyme M1/M2. Furthermore, proteins corresponding to

Table 2. Differential Protein Spots from FUdR-treated-F28-7 and -F28-7-A

spot no.	fold difference[a]	accession no.[b]	protein name	biological process (function)	theoretical pI	theoretical MW (Da)
			Spots stronger in F28-7 than in F28-7-A			
f1	1.7	P14733	Lamin B1	Chromatin modificaton	5.11	66785.60
f2[c]	5.0	P19001	Keratin, type I cytoskeletal 19 (Cytokeratin-19)	Cytoskeleton organization	5.28	44541.80
f3[d]	5.0	P19001	Keratin, type I cytoskeletal 19 (Cytokeratin-19)	Cytoskeleton organization	5.28	44541.80
f4	2.0	O35639	Annexin A3	Unknown (Calcium ion binding)	5.33	36371.00
		Q9D051	Pyruvate dehydrogenase E1 component subunit beta, mitochondrial	Glycolysis	6.41	38937.09
		Q9CSU0	Regulation of nuclear pre-mRNA domain-containing protein 1B	Unknown (Unknown)	5.73	36883.74
f5	5.0	P97861	Keratin, type II cuticular Hb6	Cytoskeleton organization	5.63	53251.26
f6	3.3	Q9D2U9	Histone H2B type 3-A	Chromosome organization	10.37	13994.20
		Q9CZX8	40S ribosomal protein S19	Translation	10.41	16085.49
f7	Specific in F28−7	Q03265	ATP synthase subunit alpha, mitochondrial	ATP biosynthesis	9.22	59752.60
		Q9CY58	Plasminogen activator inhibitor 1 RNA-binding protein	Unknown (RNA binding)	8.60	44714.12
		P50431	Serine hydroxymethyltransferase, cytosolic	Glycine metabolism	6.47	52584.87
f8	Specific in F28-7	Q03265	ATP synthase subunit alpha, mitochondrial	ATP biosynthesis	9.22	59752.60
		Q9CY58	Plasminogen activator inhibitor 1 RNA-binding protein	Unknown (RNA binding)	8.60	44714.12
f9	2.0	O35887	Calumenin	Unknown (Calcium ion binding)	4.49	37063.72
f10	2.5	O35887	Calumenin	Unknown (Calcium ion binding)	4.49	37063.72
f11	1.7	P38647	Stress-70 protein, mitochondrial (GRP 75)	Protein folding	5.91	73528.33
			Spots weaker in F28-7 than in F28-7-A			
f12	0.6	Q9R0N0	Galactokinase	Galactose metabolism	5.17	42176.08
		Q9JHJ0	Tropomodulin-3	Cytoskeleton organization	5.02	39502.72
f13	0.6	P11983	T-complex protein 1 subunit alpha B (TCP-1-alpha)	Protein folding	5.82	60448.64
		Q9R0N0	Galactokinase	Galactose metabolism	5.17	42176.08
		P02535	Keratin, type I cytoskeletal 10 (Cytokeratin-10)	Cytoskeleton organization	5.04	57769.85
		Q8R2Y8	Peptidyl-tRNA hydrolase 2, mitochondrial	Translation (Hydrolase)	6.95	19526.56
		O35639	Annexin A3	Unknown (Calcium ion binding)	5.33	36371.00
f14	0.1	Q8R2Y8	Peptidyl-tRNA hydrolase 2, mitochondrial	Translation (Hydrolase)	6.95	19526.56
f15	0.4	P11983	T-complex protein 1 subunit alpha B (TCP-1-alpha)	Protein folding	5.82	60448.64
		P42932	T-complex protein 1 subunit theta (TCP-1-theta)	Protein folding	5.44	59555.48
		P52480	Pyruvate kinase isozyme M1/M2	Glycolysis	7.17	57844.89
		Q61781	Keratin, type I cytoskeletal 14 (Cytokeratin-14)	Cytoskeleton organization	5.10	52866.97
		P80316	T-complex protein 1 subunit epsilon	Protein folding	5.72	59624.08
f16	0.5	P38647	Stress-70 protein, mitochondrial (GRP 75)	Protein folding	5.91	73528.33

[a] Fold change (FUdR-treated F28-7/FUdR-treated F28-7-A cells) > 1.5 or ≤ 0.6. [b] Swiss-prot primary accession number. [c] See graphic below. Bold-lettered peptide sequences indicate the identified peptides by MS/MS experiments in MALDI-TOF and/or nano-LC−MS/MS. [d] See graphic below. Bold-lettered peptide sequences indicate the identified peptides by MS/MS experiments in MALDI-TOF and/or nano-LC−MS/MS.

Spot No. f2

Keratin, type I cytoskeletal 19 (P19001)

MTSYSYR**QTS AMSSFGGTGG GSVRIGSGGV FRAPSIHGGS GGR**GVSVSST **RFVTSSSGSY GGVRGGSFSG TLAVSDGLLS GNEKITMQNL NDRLASYLDK VRALEQANGE LEVK**IRDWYQ KQGPGPSR**DY NHYFK**TIEDL RDK**ILGATID NSKIVLQIDN ARLAADDFRT KFETEHALRL SVEADINGLR RVLDELTLAR TDLEMQIESL KEELAYLKKN HEEEITALRS QVGGQVSVEV DSTPGVDLAK ILSEMRSQYE IMAEK**NRKDA EATYLARIEE LNTQVAVHSE QIQISKTEVT DLRRTLQGLE IELQSQLSMK AALEGTLAET EAR**YGVQLSQ IQSVISGFEA QLSDVRADIE RQNQEYKQLM DIK**SRLEQEI ATYR**SLLEGQ EAHYNNLPTP KAI

Spot No. f3

Keratin, type I cytoskeletal 19 (P19001)

MTSYSYR**QTS AMSSFGGTGG GSVRIGSGGV FR**APSIHGGS GGRGVSVSST **RFVTSSSGSY GGVRGGSFSG TLAVSDGLLS GNEKITMQNL NDRLASYLDK VRALEQANGE LEVK**IRDWYQ KQGPGPSR**DY NHYFK**TIEDL RDK**ILGATID NSKIVLQIDN ARLAADDFRT KFETEHALR**L SVEADINGLR R**VLDELTLAR** TDLEMQIESL KEELAYLKK**N HEEEITALR**S QVGGQVSVEV DSTPGVDLAK ILSEMR**SQYE IMAEK**NRK**DA EATYLAR**IEE LNTQVAVHSE QIQISK**TEVT DLR**RTLQGLE IELQSQLSMK **AALEGTLAET EAR**YGVQLSQ IQSVISGFEA QLSDVRADIE RQNQEYKQLM DIKSR**LEQEI ATYR**SLLEGQ EAHYNNLPTP KAI

chromatin and cytoskeleton-organization showed differential expressions. These proteins include lamin B1, keratin type I cytoskeletal 19 (cytokeratin-19), keratin type II cuticular Hb6, histone H2B type 3-A, keratin type I cytoskeletal 10 (cytokeratin-10), and keratin type I cytoskeletal 14 (cytokeratin-14), all of them being those involved in the maintenance of nuclear and cell morphology. Interestingly, lamin B1 and cytokeratin-19 were higher (1.7, 5.0, respectively) in F28-7 (necrosis cells), compared to F28-7-A cells (apoptosis cells) in this FUdR-treatment (Table 2 and Figure 3). At the untreated stage also,

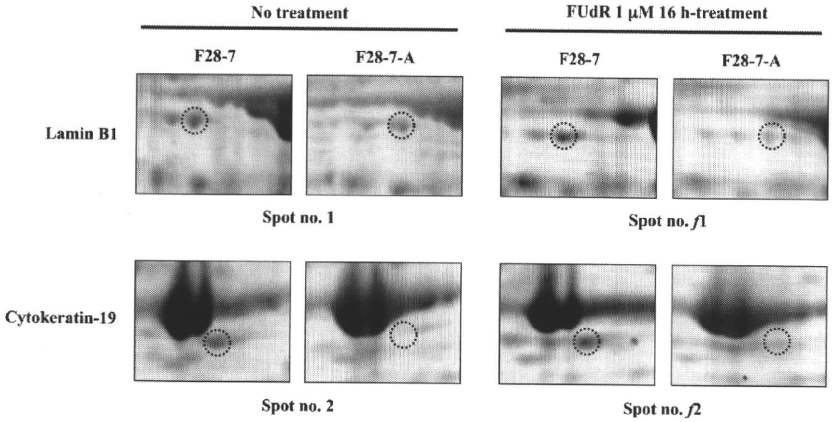

Figure 3. Selected regions of two-dimensional gels illustrating individual protein expression changes following FUdR treatment. Pictures showing enlarged areas for lamin B1 (spot 1 and spot *f*1), and cytokeratin-19 (spot 2 and spot *f*2).

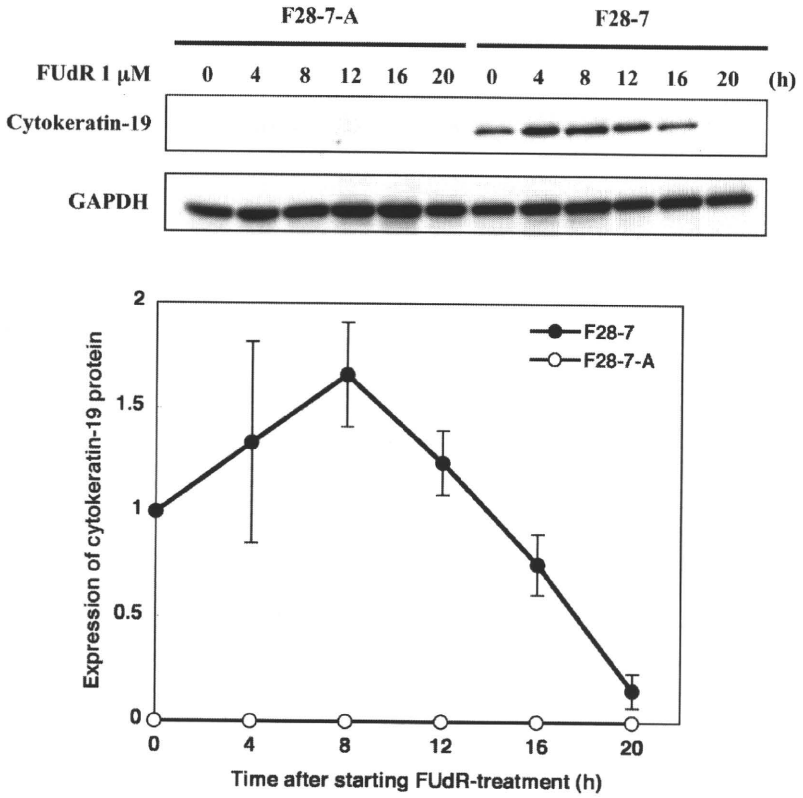

Figure 4. Western blot validation of cytokeratin-19 protein expression. Whole cell lysates were prepared from F28-7 and F28-7-A cells in untreated (0 h) and FUdR-treated stages (4, 8, 12, 16 h). Expression of cytokeratin-19 and GAPDH proteins were examined by Western blot analysis. Expression of GAPDH was used as an internal control. The patterns shown are results obtained in one experiment. Two additional experiments gave similar results. Expression of cytokeratin-19 protein is represented by the density of cytokeratin-19/GAPDH protein band relative to the zero-time value with F28-7 cells (●). The values for F28-7-A (○) were null at all data points. Results are averages of three independent experiments with error bars showing the ±SD in triplicates.

lamin B1 and cytokeratin-19 were higher (2.5, and 3.3, respectively) in F28-7, compared to F28-7-A (Table 1 and Figure 3). Therefore, we interpreted this as suggesting that lamin B1 and cytokeratin-19 could be regulators in the FUdR-induced necrosis and apoptosis.

Modulation of FUdR-Induced Cell Death by Silencing Cytokeratin-19 Expression. As described above, lamin B1 and cytokeratin-19 are strongly expressed in F28-7, as compared with those in F28-7-A, both in untreated- and FUdR-treated-stages. Our previous work showed that the knockdown of lamin B1 by siRNA technique can cause a shift from FUdR-induced necrosis to apoptosis.[8] In addition, we previously reported that the cytokeratin-19 mRNA was strongly expressed in FUdR-induced necrosis, as compared with those in FUdR-induced apoptosis, by using cDNA microarray technology.[6] The possibility that cytokeratin-19 may also be associated with these differential patterns of cell death morphology was, therefore, investigated.

First, we analyzed the expression levels of cytokeratin-19, using Western blotting. As shown in Figure 4, the cytokeratin-19 protein was detected for F28-7 but not for F28-7-A cells. The level of cytokeratin-19 protein was indeed higher in F28-7 than in F28-7-A both before and after the FUdR-treatment. In the F28-7 cells, the expression of cytokeratin-19 protein

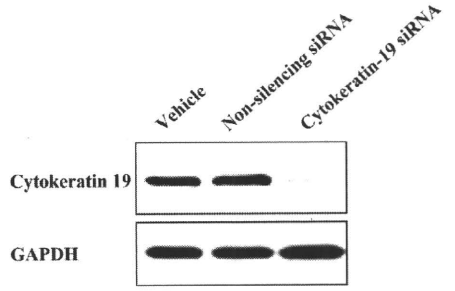

Figure 5. Knockdown of cytokeratin-19 by RNA interference. F28-7 cells were transfected with nonsilencing siRNA and with cytokeratin-19 siRNA cocktail. Forty-eight hours after the transfection, the levels of expression of cytokeratin-19 and those of GAPDH, an internal control, were examined by Western blot analysis. These results are representative of three independent experiments.

continued to increase until eight-hours of the FUdR-treatment, then decreased gradually, until it reached near to the zero level at 20 h.

Next, to test if a lowering of endogenously expressed cytokeratin-19 in F28-7 cells can modulate FUdR-induced necrosis, we carried out a knockdown of the expression in F28-7 cells by using cytokeratin-19 siRNA. Western blot analysis performed for cell extracts at 48 h after the siRNA-transfection at a greater-than-80% efficiency indicated that the treatment reduced the cytokeratin-19 protein levels, while the glyceraldehyde-3-phosphate dehydrogenase (GAPDH) protein levels as a control showed no change (Figure 5). The level of cytokeratin-19 protein expression in F28-7 became as low as that in F28-7-A cells. Thus, the knockdown efficacy was more than 70% in cytokeratin-19 siRNA cocktail-transfected cells, compared to that in the vehicle- and nonsilencing siRNA-transfected cells. Another control experiment in which a nonsilencing siRNA was administered showed no effect on the expression of cytokeratin-19 or GAPDH. The cell viability at 48 h after the transfection was 95.5 ± 0.9% ($n = 3$) with the vehicle, 98.9 ± 0.7% ($n = 3$) with the nonsilencing siRNA, and 99.1 ± 0.6% ($n = 3$) in the cytokeratin-19 siRNA cocktail-transfected cells. The knockdown of cytokeratin-19 in the F28-7 cells did not change the cell viability. In addition, either the nonsilencing siRNA or the cytokeratin-19 siRNA cocktail alone had no effect on the cell morphology, that is, the morphology-change required subsequent FUdR-treatment (Figure 6, upper diagram).

We explored the morphology in the cytokeratin-19 knocked-down F28-7 cells on treatment with 1 μM FUdR. The necrotic morphology in F28-7 and apoptotic morphology in F28-7-A cells were characteristically observed at 21 h after treatment with FUdR. At the 21 h, the controls given vehicle or nonsilencing siRNA showed the cytoplasmic swelling, a feature of necrosis, and the cytokeratin-19 siRNA cocktail-transfected cells, in contrast, showed a typical apoptotic morphology; the membrane blebbing and the formation of apoptotic bodies (Figure 6, bottom diagram). At this point of treatment, the cell viability was 26.7 ± 1.6% ($n = 3$) with the vehicle, 26.6 ± 1.9% ($n = 3$) with the nonsilencing siRNA, and 28.0 ± 1.1% ($n = 3$) with the cytokeratin-19 siRNA cocktail transfection. These results indicate that the knockdown of cytokeratin-19 caused the cells a shift from necrosis to apoptosis, without changing the viability-levels. We confirmed, by microscopic inspection, that almost all the dying cells underwent apoptotic morphologies after the cytokeratin-19 siRNA cocktail transfection with subsequent FUdR treatment.

Discussion

We believe that depending on intracellular environment, for example proteome status, a cell is destined to necrosis or to apoptosis. Our previous reports to sort out candidate regulators for the cell death-pathways from the microarray data, however, have been unsuccessful.[6] This time, with the use of proteome analysis, we have shown that at the untreated and FUdR-treated stages the nuclear and the cytoplasmic intermediate filament-proteins, lamin B1 and cytokeratin-19, are higher in F28-7 than in F28-7-A cells. Consequently, we focused on these proteins as candidate cell death-regulators of FUdR-induced necrosis and apoptosis. Thus, in our recent publication,[8] we reported that a knockdown of lamin B1 by its siRNA induced a shift from necrosis to apoptosis in F28-7 cells, thereby proposing that lamin B1 could be such a regulator. Lamin B1 is one of the nuclear lamins and a key structural component of the lamina, an intermediate filament meshwork that lies beneath the inner nuclear membrane. It is known that the nuclear lamins play a crucial role in fundamental cellular processes, including nuclear organization, chromatin segregation, DNA

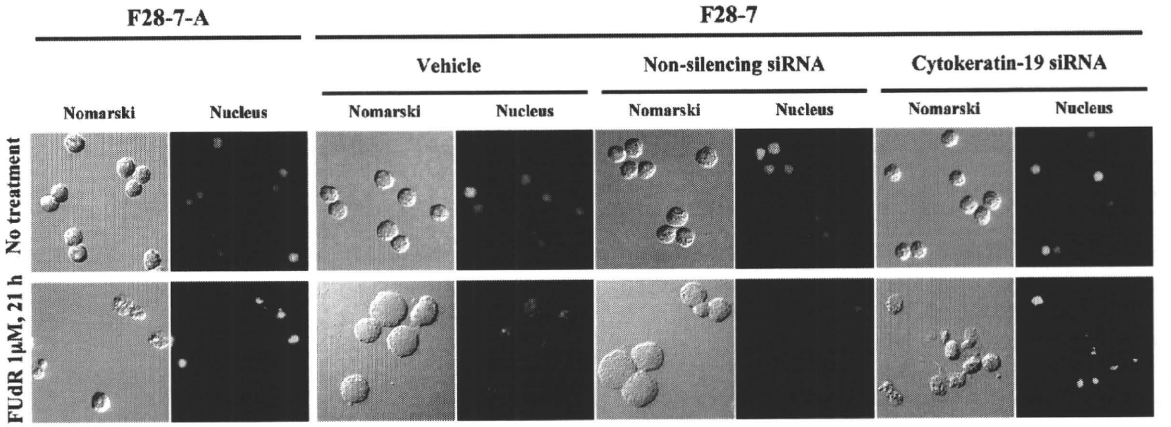

Figure 6. Knockdown of cytokeratin-19 shifts FUdR-induced cell-death morphology from necrosis to apoptosis. Forty-eight hours after transfection with the vehicle, the nonsilencing siRNA, or the cytokeratin-19 siRNA cocktail, the F28-7 cells were treated with or without 1 μM FUdR for 21 h and then stained with DAPI as described under Materials and Methods. Morphological changes were analyzed under a fluorescence microscope at ×400 magnification. Two additional experiments gave similar results.

replication, and gene expression.[9−13] Using the same strategy as with lamin B1, we have shown here that a knockdown of cytokeratin-19 in F28-7 results in a shift from necrosis to apoptosis for the FUdR-induced cell-death, leading us to propose that cytokeratin-19 functions, either directly or indirectly, in regulating the cell death-morphology. Both of those proteins, lamin B1 and cytokeratin-19, are constituents of cellular intermediate filaments. Intermediate filaments, together with actin microfilaments and tublin microtubles, comprise the three major cytoskeletal networks that are found in most eukaryotic cells.[14] Keratins, which are the largest intermediate filament protein subgroup, can be divided into acidic type-I (K9−K20) and basic type-II (K1−K8).[15] Keratin networks are highly dynamic; keratins are reorganized during cell differentiation, mitosis and apoptosis, and they play important cytoprotective and structural support roles for the cells.[16,17] Cytokeratin-19 is a member in the largest cytoplasmic intermediate filament-protein subgroup, constituting a key structural component of the cytoskeletal proteins.[18,19] Previous reports have indicated that cytokeratin-19 undergoes caspase-mediated degradation during apoptosis.[20−22] However, participation of cytokeratin-19 in regulation of necrosis and apoptosis has not been documented. Our data suggest that strong expressions of nuclear and cytoplasmic intermediate filament-proteins, lamin B1 and cytokeratin-19, are important in necrosis, and poor expressions of these proteins lead to apoptosis. In addition, it is known that nuclear and cytoplasmic intermediate filament-proteins (e.g., lamin B1, cytokeratin-8, cytokeratin-18, cytokeratin-19, and vimentin) are caspase substrates, which undergo caspase-mediated cleavage during apoptosis.[20−24] It seems that a decrease of these intermediate filament-proteins gives greater flexibility in nucleus and cell-structure, thereby leading to apoptosis.

As described above, the proteome analysis revealed differently expressed proteins (see Tables 1 and 2). Most of these proteins are for the first time revealed as being differently expressed in necrosis and apoptosis. These proteins need to be investigated further to determine whether they are directly involved in the FUdR-induced necrosis and apoptosis at all.

In our proteome analysis, several proteins (e.g., stress-70 protein, galactokinase, annexin A3 and ATP synthase subunit alpha) were detectable in different spots, most likely as a consequence of post-translational modifications or differential mRNA splicings.

Our recent work revealed that a release of cytochrome c from mitochondria into the cytoplasm and nucleus occurs in the apoptosis but not in the necrosis.[6] Reports from other laboratories have shown that mitochondria play a role in mediating both necrosis and apoptosis.[25−27] Interestingly, a number of the mitochondrial proteins exhibit differential expressions in F28-7 and F28-7-A cells either in the untreated stages or in the FUdR-treated stages. Among these proteins, a member of the molecular chaperone Heat shock protein 70 (HSP70) family, stress-70 protein (GRP75), was found to be present in Spot 4 in Figure 1A and Spot 7 in Figure 1B. It is known that GRP75 receives phosphorylation and/or acetylation as post-translational modifications.[28,29] We propose that an expression change, that can involve post-translational modification, of these mitochondria-localized proteins play an important role prior to the release of cytochrome c, a role decisive in determining the FUdR-induced death morphology.

Previously, we demonstrated that an inhibition of HSP90, a well-documented chaperone, causes in F28-7 a shift from necrosis to apoptosis in FUdR-induced cell-killing.[6] HSP90 is probably one of key regulators in the necrosis and apoptosis, and it would be interesting to explore the relationship between the presently found activities of cytokeratin-19 and lamin B1, the filament constituents, and the role of the ubiquitous cell-component HSP90 in the cell death.

Finally, our present work shows that these cell-death models and the approach by proteome analysis coupled with usage of interfering RNAs provide a useful methodology in studying molecular mechanisms of necrosis and apoptosis.

Acknowledgment. We thank Dr. Hikoya Hayatsu (Faculty of Pharmaceutical Sciences, Okayama University) for helpful discussions. This research was partly supported by Grant-in-Aid for Young Scientists (B) from the Ministry of Education, Culture, Sports, Science and Technology (21790078, A.S.).

Supporting Information Available: Supplementary Figure 1 and Tables 1−3. This material is available free of charge via the Internet at http://pubs.acs.org.

References

(1) Klose, J.; Kobalz, U. Two-dimensional electrophoresis of proteins: an updated protocol and implications for a functional analysis of the genome. *Electrophoresis* **1995**, *16*, 1034–1059.
(2) Farber, E. Programmed cell death: necrosis versus apoptosis. *Mod. Pathol.* **1994**, *7*, 605–609.
(3) Kerr, J. F. Shrinkage necrosis: a distinct mode of cellular death. *J. Pathol.* **1971**, *105*, 13–20.
(4) Thiede, B.; Rudel, T. Proteome analysis of apoptotic cells. *Mass Spectrom. Rev.* **2004**, *23*, 333–349.
(5) Kakutani, T.; Ebara, Y.; Kanja, K.; Hidaka, M.; et al. Different modes of cell death induced by 5-fluoro-2′-deoxyuridine in two clones of the mouse mammary tumor FM3A cell line. *Biochem. Biophys. Res. Commun.* **1998**, *247*, 773–779.
(6) Sato, A.; Hiramoto, A.; Uchikubo, Y.; Miyazaki, E.; et al. Gene expression profiles of necrosis and apoptosis induced by 5-fluoro-2′-deoxyuridine. *Genomics* **2008**, *92*, 9–17.
(7) Yoshioka, A.; Tanaka, S.; Hiraoka, O.; Koyama, Y.; et al. Deoxyribonucleoside triphosphate imbalance. 5-Fluorodeoxyuridine-induced DNA double strand breaks in mouse FM3A cells and the mechanism of cell death. *J. Biol. Chem.* **1987**, *262*, 8235–8241.
(8) Sato, A.; Hiramoto, A.; Satake, A.; Miyazaki, E.; et al. Association of nuclear membrane protein lamin B1 with necrosis and apoptosis in cell death induced by 5-fluoro-2′-deoxyuridine. *Nucleosides Nucleotides Nucleic Acids* **2008**, *27*, 433–438.
(9) Cohen, M.; Lee, K. K.; Wilson, K. L.; Gruenbaum, Y. Transcriptional repression, apoptosis, human disease and the functional evolution of the nuclear lamina. *Trends Biochem. Sci.* **2001**, *26*, 41–47.
(10) Wilson, K. L.; Zastrow, M. S.; Lee, K. K. Lamins and disease: insights into nuclear infrastructure. *Cell* **2001**, *104*, 647–650.
(11) Goldman, R. D.; Gruenbaum, Y.; Moir, R. D.; Shumaker, D. K.; et al. Nuclear lamins: building blocks of nuclear architecture. *Genes Dev.* **2002**, *16*, 533–547.
(12) Burke, B.; Stewart, C. L. Life at the edge: the nuclear envelope and human disease. *Nat. Rev. Mol. Cell Biol.* **2002**, *3*, 575–585.
(13) Hutchison, C. J. Lamins: building blocks or regulators of gene expression. *Nat. Rev. Mol. Cell Biol.* **2002**, *3*, 848–858.
(14) Ku, N. O.; Zhou, X.; Toivola, D. M.; Omary, M. B. The cytoskeleton of digestive epithelia in health and disease. *Am. J. Physiol.* **1999**, *277*, G1108–1137.
(15) Schweizer, J.; Bowden, P. E.; Coulombe, P. A.; Langbein, L.; et al. New consensus nomenclature for mammalian keratins. *J. Cell Biol.* **2006**, *174*, 169–174.
(16) Omary, M. B.; Coulombe, P. A.; McLean, W. H. Intermediate filament proteins and their associated diseases. *N. Engl. J. Med.* **2004**, *351*, 2087–2100.

(17) Omary, M. B.; Ku, N. O.; Tao, G. Z.; Toivola, D. M.; et al. Heads and tails" of intermediate filament phosphorylation: multiple sites and functional insights. *Trends Biochem. Sci.* **2006**, *31*, 383–394.
(18) Wu, Y. J.; Rheinwald, J. G. A new small (40 kd) keratin filament protein made by some cultured human squamous cell carcinomas. *Cell* **1981**, *25*, 627–635.
(19) Moll, R.; von Bassewitz, D. B.; Schulz, U.; Franke, W. W. An unusual type of cytokeratin filament in cells of a human cloacogenic carcinoma derived from the anorectal transition zone. *Differentiation* **1982**, *22*, 25–40.
(20) Ku, N. O.; Liao, J.; Omary, M. B. Apoptosis generates stable fragments of human type I keratins. *J. Biol. Chem.* **1997**, *272*, 33197–33203.
(21) Ku, N. O.; Omary, M. B. Effect of mutation and phosphorylation of type I keratins on their caspase-mediated degradation. *J. Biol. Chem.* **2001**, *2276*, 26792–26798.
(22) Oshima, R. G. Apoptosis and keratin intermediate filaments. *Cell Death Differ.* **2001**, *9*, 486–492.
(23) Kawahara, A.; Enari, M.; Talanian, R. V.; Wong, W. W.; et al. Fas-induced DNA fragmentation and proteolysis of nuclear proteins. *Genes Cells* **1998**, *3*, 297–306.
(24) Byun, Y.; Chen, F.; Chang, R.; Trivedi, M.; et al. Caspase cleavage of vimentin disrupts intermediate filaments and promotes apoptosis. *Cell Death Differ.* **2001**, *8*, 443–450.
(25) Tsujimoto, Y. Cell death regulation by the Bcl-2 protein family in the mitochondria. *J. Cell. Physiol.* **2003**, *195*, 158–167.
(26) Green, D. R.; Kroemer, G. The pathophysiology of mitochondrial cell death. *Science* **2004**, *305*, 626–629.
(27) Nakagawa, T.; Shimizu, S.; Watanabe, T.; Yamaguchi, O.; et al. Cyclophilin D-dependent mitochondrial permeability transition regulates some necrotic but not apoptotic cell death. *Nature* **2005**, *434*, 652–658.
(28) Rikova, K.; Guo, A.; Zeng, Q.; Possemato, A.; et al. Global survey of phosphotyrosine signaling identifies oncogenic kinases in lung cancer. *Cell* **2007**, *131*, 1190–1203.
(29) Matsuoka, S.; Ballif, B. A.; Smogorzewska, A.; McDonald, E. R.; et al. ATM and ATR substrate analysis reveals extensive protein networks responsive to DNA damage. *Science* **2007**, *316*, 1160–1166.

PR9010537

Transmission of the bacterium occurs primarily through bites from arthropods, including the dog tick (*Dermacentor variabilis*), the wood tick (*D. andersoni*), the lone star tick (*Amblyomma americanum*), and the deer fly (*Chrysops* spp.). In addition, contact with infected animals, most commonly rabbits, wild rodents, and cats, is another common route of transmission to humans (*1,6*).

Tularemia occurs in various animal species. Lagomorphs, rodents, and sheep are most susceptible; infected animals are frequently found dead or moribund. Carnivores are less susceptible; however, feline tularemia occurs sporadically, and human infections associated with bites and scratches from infected cats have been recognized (*7*). In addition to arthropod bites, contact with infected dead rabbits or their tissues appears to be the most common source of human infection. A wide variety of case reports have been published describing unique incidences of rabbit–human transmission, including a lawn mower aerosolizing rabbit nests along with their occupants (*8*), consumption of undercooked rabbit meat (*9*), and contact with a "lucky" rabbit's foot (*10*).

The purpose of this report is to alert veterinarians, veterinary laboratory personnel, and public health officials that rabbit tularemia can be easily overlooked on gross examination in animals displaying lesions of hepatic coccidiosis, a common disease of the wild rabbit. Therefore, all rabbits submitted for postmortem examinations should be regarded as potentially infected with tularemia, particularly during seasons when vectors are active.

Dae Young Kim, Thomas J. Reilly, Susan K. Schommer, and Sean T. Spagnoli

Author affiliation: University of Missouri, Columbia, Missouri, USA

DOI: 10.3201/eid1612.101013

References

1. Foley JE, Nieto NC. Tularemia. Vet Microbiol. 2010;140:332–8. DOI: 10.1016/j.vetmic.2009.07.017
2. Hobbs RP, Twigg LE. Coccidia (*Eimeria* spp.) of wild rabbits in southwestern Australia. Aust Vet J. 1998;76:209–10. DOI: 10.1111/j.1751-0813.1998.tb10131.x
3. Ellis J, Oyston PC, Green M, Titball RW. Tularemia. Clin Microbiol Rev. 2002;15:631–46. DOI: 10.1128/CMR.15.4.631-646.2002
4. Long GW, Oprandy JJ, Narayanan RB, Fortier AH, Porter KR, Nacy CA. Detection of *Francisella tularensis* in blood by polymerase chain reaction. J Clin Microbiol. 1993;31:152–4.
5. Centers for Disease Control and Prevention. Reported tularemia cases by state—United States, 2000–2008 [cited 2010 Jun 23]. http://www.cdc.gov/tularemia/Surveillance/Tul_CasesbyState.html
6. Farlow J, Wagner DM, Dukerich M, Stanley M, Chu M, Kubota K, et al. *Francisella tularensis* in the United States. Emerg Infect Dis. 2005;11:1835–41.
7. Arav-Boger R. Cat-bite tularemia in a seventeen-year-old girl treated with ciprofloxacin. Pediatr Infect Dis J. 2000;19:583–4. DOI: 10.1097/00006454-200006000-00024
8. Agger WA. Tularemia, lawn mowers, and rabbits' nests. J Clin Microbiol. 2005;43:4304. DOI: 10.1128/JCM.43.8.4304-4305.2005
9. Jansen A, Schmidt W, Schneider T. Rabbit's revenge. Lancet Infect Dis. 2003;3:348. DOI: 10.1016/S1473-3099(03)00656-X
10. Ryan-Poirier K, Whitehead PY, Leggiadro RJ. An unlucky rabbit's foot? Pediatrics. 1990;85:598–600.

Address for correspondence: Dae Young Kim, Veterinary Medical Diagnostic Laboratory, College of Veterinary Medicine, University of Missouri, 1600 E Rollins St, Columbia, MO 65211, USA; email: kimdy@missouri.edu

Imported Leishmaniasis in Dogs, US Military Bases, Japan

To the Editor: Leishmaniasis is found in canids in ≈50 of the 88 countries where leishmaniases are found in humans (*1*). In Japan, 2 cases of imported canine leishmaniasis have been documented in dogs from Spain (*2,3*). We report 2 cases of leishmaniasis in dogs in which dermatitis developed mainly on the face. Leishmaniasis was diagnosed from results of a serologic rk39 test, followed by PCR of skin lesion specimens for the *Leishmania* spp.–specific small subunit (SSU) rRNA gene. Because the dogs had lived on a US military base in Sicily, Italy, for 3 years before their owners were transfered to Japan, the animals were likely infected with *L. infantum* in Italy.

Animal 1 was a 6-year-old female dog that had lived in Sicily for 3 years, since 2003, and had been brought to Japan in September 2006. While she lived in Italy, she had exhibited alopecic, pruritic, and crusty skin lesions, mainly around the face and on the forearms and hind legs.

In November 2006, the dog was brought to the US Army Veterinary Command's Zama Veterinary Treatment Facility with dermatitis (online Appendix Figure, panel A, www.cdc.gov/EID/content/16/12/2017-appF.htm) and additional signs of kidney failure. A serum specimen was positive by the rk39 dipstick test for diagnosis of visceral leishmaniasis (Kalazar Detect; InBios, Seattle, WA, USA). A skin punch biopsy specimen was obtained for cultures and PCR for the parasites in December 2006. Cultures of 4 skin specimens were all negative, probably because of cool transportation of the samples for 1.5 days before the cultures were started. The dog's condition was treated with ketoconazole and then allopurinol. The

skin conditions initially improved, but the lesions did not completely resolve (online Apendix Figure, panels B–D). In May 2008, the dog was humanely killed because of central vestibular disease with unknown cause. A necropsy was not performed.

Animal 2 was a 12-year-old male dog that had also lived in Sicily for 3 years since 2000, and was brought to Yokosuka Base in Japan in 2003. In January 2004, the dog was positive for visceral leishmaniasis by the rk39 test; no particular clinical signs were observed.

In March 2007, the dog was referred to Zama Veterinary Treatment Facility with pruritic alopecia on the dorsum and head, and a skin punch biopsy specimen was obtained for histopathologic evaluation. The presence of amastigotes of *Leishmania* species within areas of dermal inflammation was confirmed at the Armed Forces Institute of Pathology (Washington, DC, USA). In April 2007, a second skin punch biopsy specimen was obtained for PCR.

PCR was performed for the *Leishmania*-specific SSU rRNA gene (*4*). For primary PCR, primers R221 (5′-GGTTCCTTTCCTGATTTACG-3′) and R332 (5′-GGCCGGTAAAGGCC GAATAG-3′) were used. For nested PCR, primers R223 (5′-TCCCA TCGCAACCTCGGTT-3′) and R333 (5′-AAAGCGGGCGCGGTG CTG-3′) were used. In the primary reaction, the expected PCR products of ≈603 bp were detected in 2 of 4 skin DNA specimens from patient 1 and 1 of 5 skin DNA specimens from patient 2 (Figure, panel A, lanes 2, 3, 9). In the nested reaction, the expected PCR products of ≈359 bp were seen in all 4 specimens from patient 1 and in 4 of 5 specimens from patient 2 (Figure, panel B, lanes 1–4, and 5, 6, 8, 9); some bands were faint. The nucleotide sequences (288 bp) of the nested PCR product of patient 1 were 100% identical to those of patient 2 and sequences of the SSU rRNA gene of *L. infantum* (IPT1 strain, used as a positive control), *L. infantum* (M81429), *L. donovani* (M80295), and *L. chagasi* (M81430).

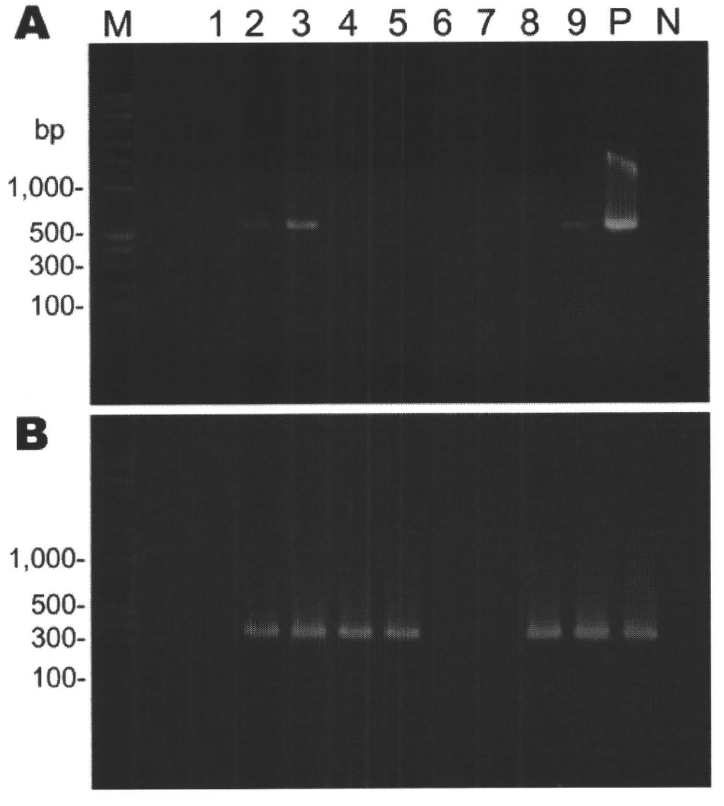

Figure. PCR amplification of the *Leishmania* spp.–specific small subunit rRNA gene from skin biopsy specimens from infected dogs, Japan. DNA samples (100–200 ng) were subjected to primary PCR (A), followed by nested PCR (B). Lanes 1–4, skin DNA samples from patient 1; lanes 5–9, skin DNA samples from patient 2; M, DNA molecular marker; P, positive control; N, negative control.

Global warming, which causes changes in the distribution of the sand fly vectors, and human-produced risk factors, such as travel, migration, and urbanization, may increase the incidence of leishmaniasis (*5*). Military mobility and operations are also a major risk factor for leishmaniasis in humans and canids (*6*). In Japan, of >300 kala-azar (visceral leishmaniasis) patients reported, 218 were soldiers who returned from the People's Republic of China before and after World War II (*7*). In the present study, 2 dogs infected with *L. infantum* had been brought to Japan from Italy by US military families.

Dog-to-dog transmission by direct contact with contaminated blood through biting may explain the recent outbreaks of leishmaniasis in foxhounds in North America (*8*). In Japan, although no sandfly species that could transmit leishmania have been reported (*7*), direct dog-to-dog transmission of leishmaniasis can occur. *Babesia gibsoni* infection is prevalent among fighting dogs in Japan, likely because of the transmission of infected erythrocytes through biting (*9*). Greater sharing of information and of diagnostic procedures is required in Japan because few medical and veterinary practitioners have experience with leishmaniasis patients.

This study was supported in part by grants from the Global Center of Excellence program for International Collaboration Centers for Zoonosis Control and grant no. 183801780 from the Ministry

of Education, Culture, Sport, Science and Technology of Japan.

Yuta Kawamura, Isao Yoshikawa, and Ken Katakura

Author affiliations: Hokkaido University Graduate School of Veterinary Medicine, Sapporo, Hokkaido, Japan (Y. Kawamura, K. Katakura); and US Army Japan District Veterinary Command–Zama Branch Kangawa, Japan (I. Yoshikawa)

DOI: 10.3201/eid1612.100389

References

1. Alvar J, Cañavate C, Molina R, Moreno J, Nieto J. Canine leishmaniasis. Adv Parasitol. 2004;57:1–88. DOI: 10.1016/S0065-308X(04)57001-X
2. Namikawa K, Watanabe M, Lynch J, Sugaki Y, Kitai T, Sunaga F, et al. A canine case of *Leishmania infantum* infection in Japan. Jpn J Vet Dermatol. 2006;12:11–5. DOI: 10.2736/jjvd.12.11
3. Takahashi N, Naya T, Watari T, Matsumoto Y, Matsumoto Y, Tsujimoto H, et al. An imported case of canine cutaneous leishmaniasis in Japan. Jpn J Vet Dermatol. 1997;3:25–7.
4. Van Eys GJ, Schoone GJ, Kroon NC, Ebeling SB. Sequence analysis of small subunit ribosomal RNA genes and its use for detection and identification of *Leishmania* parasites. Mol Biochem Parasitol. 1992;51:133–42. DOI: 10.1016/0166-6851(92)90208-2
5. Desjeux P. The increase in risk factors for leishmaniasis worldwide. Trans R Soc Trop Med Hyg. 2001;95:239–43. DOI: 10.1016/S0035-9203(01)90223-8
6. Coleman RE, Bukert DA, Putma JL, Sherwood V, Caci JB, Jennings BT, et al. Impact of Phlebotomine sand flies on U.S. military operations at Talli air base, Iraq: 1. background, military situation, and development of a "leishmaniasis control program." J Med Entomol. 2006;43:647–62. DOI: 10.1603/0022-2585(2006)43[647:IOPSFO]2.0.CO;2
7. Katakura K. Molecular epidemiology of leishmaniasis in Asia (focus on cutaneous infections). Curr Opin Infect Dis. 2009;22:126–30. DOI: 10.1097/QCO.0b013e3283229ff2'
8. Duprey ZH, Steurer FJ, Rooney JA, Kirchhoff LV, Jackson JE, Rowton ED, et al. Canine visceral leishmaniasis, United States and Canada, 2000–2003. Emerg Infect Dis. 2006;12:440–6.
9. Miyama T, Sakata Y, Shimada Y, Ogino S, Watanabe M, Itamoto K, et al. Epidemiological survey of *Babesia gibsoni* infection in dogs in eastern Japan. J Vet Med Sci. 2003;67:467–71. DOI: 10.1292/jvms.67.467

Address for correspondence: Ken Katakura, Laboratory of Parasitology, Department of Disease Control, Graduate School of Veterinary Medicine, Hokkaido University, Kita 18 Nishi 9, Kita-ku Sapporo 060-0818, Hokkaido, Japan; email: kenkata@vetmed.hokudai.ac.jp

Serologic Evidence of Pandemic (H1N1) 2009 Infection in Dogs, Italy

To the Editor: Until recently, the general consensus has been that dogs are poorly susceptible to natural infection with influenza A viruses; however, since the recent upsurge of influenza A circulating subtypes H5N1 and H1N1 viruses, cases of natural infection in dogs have apparently increased. Thus, the role of these animals is being reconsidered in the transmission and spread of influenza viruses (*1–3*).

In April 2009, the most recent of the human influenza A pandemics, pandemic (H1N1) 2009, was detected in Mexico. The virus rapidly spread worldwide, within weeks of its first isolation. To date, pandemic (H1N1) 2009 has primarily infected humans, although transmission from infected humans to other animals, including pigs, turkeys, ferrets, cats, and dogs has been reported (*4,5*).

In Italy (population ≈58 million), the first human cases of pandemic (H1N1) 2009 were reported in May 2009; confirmed cases peaked during the second week of November 2009 (week 46) (*6*). As of May 9, 2010, Italy had recorded an estimated 5,582,000 cases of pandemic (H1N1) 2009. In Italy as well, the population has ≈7 million companion dogs and ≈7.5 million cats (*7*). Because of the close contact between persons and their companion animals, we initiated this serologic study to determine whether evidence of pandemic (H1N1) 2009 transmission could be found in companion animals in Italy.

We tested serum specimens from dogs (n = 964) and cats (n = 97), originally submitted to the Istituto Zooprofilattico Sperimentale delle Venezie in Legnaro, Italy, from October through December 2009 (weeks 41–53), for assessment of rabies vaccine efficacy. An average of 70 samples were tested per week; the highest number of samples (n = 106) was tested for week 51 and the lowest (n = 25) for week 53. Testing for antibody to influenza A nucleoprotein was performed by using a commercially available competitive ELISA (cELISA) (ID Screen Influenza A Antibody Competition Assay; ID Vet, Montpellier, France), according to the manufacturer's instructions. Previous work from our laboratory has assigned a sensitivity of 93.98% and specificity of 98.71% to this cELISA for the testing of canine serum samples (*8*). In total, 29 serum specimens tested at a 1:10 dilution, all from dogs, were positive after a second confirmatory screening. None of the 97 feline serum samples were positive by cELISA.

The cELISA-positive serum specimens were then treated with receptor-destroying enzyme (RDE; Sigma-Aldrich, St. Louis, MO, USA) (1 part serum: 3 parts RDE) for 16 h at 37°C, followed by heat inactivation at 56°C for 30 min. We then tested the specimens by the hemagglutination inhibition (HI) test against the pandemic virus A/Verona/Italy/2810/2009 (H1N1), A/swine/Italy/711/2006 (H1N1), and H3N8 (A/canine/Florida/2004) by using 0.5% chicken erythrocytes and standard methods (*9*). Seven serum samples (nos. 4410, 4438, 4444, 4460, 4517, 4520, 4681) were positive by HI

NOTE *Parasitology*

Evaluation of Myanmar Medicinal Plant Extracts for Antitrypanosomal and Cytotoxic Activities

Saw BAWM[1], Saruda TIWANANTHAGORN[1], Kyaw San LIN[2], Junichi HIROTA[1], Takao IRIE[1], Lat Lat HTUN[2], Ni Ni MAW[3], Tin Tin MYAING[2], Nyunt PHAY[4], Satoshi MIYAZAKI[1], Tatsuya SAKURAI[1], Yuzaburo OKU[1], Hideyuki MATSUURA[5] and Ken KATAKURA[1]*

[1]*Laboratory of Parasitology, Department of Disease Control, Graduate School of Veterinary Medicine, Hokkaido University, Kita 18, Nishi 9, Kita-ku, Sapporo 060–0818, Japan,* [2]*Department of Pharmacology and Parasitology, University of Veterinary Science, Yezin, Naypyitaw, Myanmar,* [3]*Livestock Breeding and Veterinary Department, Naypyitaw, Myanmar,* [4]*Pathein University, Pathein, Myanmar and* [5]*Laboratory of Bioorganic Chemistry, Division of Applied Bioscience, Graduate School of Agriculture, Hokkaido University, Kita 9, Nishi 9, Kita-ku, Sapporo 060–8589, Japan*

(Received 11 November 2009/Accepted 6 December 2009/Published online in J-STAGE 22 December 2009)

ABSTRACT. Current chemotherapeutic options for African trypanosomiasis in humans and livestock are very limited. In the present study, a total of 71 medicinal plant specimens from 60 plant species collected in Myanmar were screened for antitrypanosomal activity against trypomastigotes of *Trypanosoma evansi* and cytotoxicity against MRC-5 cells *in vitro*. The methanol extract of dried rootbark of *Vitis repens* showed the highest antitrypanosomal activity with IC_{50} value of 8.6 ± 1.5 μg/ml and the highest selectivity index of 24.4. The extracts of *Brucea javanica, Vitex arborea, Eucalyptus globulus* and *Jatropha podagrica* had also remarkable activity with IC_{50} values and selectivity indices in the range of 27.2–52.6 μg/ml and 11.4–15.1 respectively.

KEY WORDS: antitrypanosomal activity, Myanmar medicinal plants, *Trypanosoma evansi*, *Vitis repens*.

J. Vet. Med. Sci. 72(4): 525–528, 2010

Tsetse-transmitted African trypanosomiasis, such as sleeping sickness in humans and nagana in cattle, are causing serious problems to human health and animal production in Africa. A wasting disease called surra by *Trypanosoma evansi* infection is not restricted to Africa and distributed worldwide, because the parasite is mechanically transmitted by blood-sucking insects such as *Tabanus* and *Stomoxys* species. *T. evansi* is pathogenic to a wide variety of animals, including equines, camels, cattle, buffaloes, goats, sheep, pigs, and dogs, causing great economic losses in livestock industries in Asia [3, 9]. However, current chemotherapeutic options for trypanosomiasis in humans and livestock are very limited and far from ideal. Existing trypanocidal drugs have to be administered by injection. The drugs have been associated with severe side-effects and ineffectiveness against drug resistant parasites. Therefore, research for developing of new drugs, which are safe, effective, cheap, easy-to-administer, and possess novel mechanism of action, is urgently needed [6, 7, 10].

Myanmar is abundant plant resources and Myanmar peoples have inherited their own traditional medicine to maintain their health and treat various ailments including malaria, diarrhea and fever for over millennia of history [14]. Recently, we reported that quassinoids isolated from the fruits of an Asian medicinal plant, *Brucea javanica*, showed remarkable antibabesial and antitrypanosomal activities [2, 11, 16], suggesting a promise use of medicinal plant extracts for protozoan diseases in livestock. In the present study, the *in vitro* antitrypanosomal and cytotoxic activities of crude extracts of medicinal plants in Myanmar were evaluated.

A total of 55 fresh plant specimens from 45 plant species were collected at the National Herbal Park in Naypyitaw and the National Botanical Garden in Pyin-oo-lwin, Myanmar in January 2009 (Table 1). Species identification was done by Mr. Hla Myint and Dr. Kyaw Kyaw Swe at each Institute. These fresh plants were cut into small pieces with scissors and preserved in 70% ethanol immediately after collection. Seven dry plant specimens from seven plant species were prepared at Pathein University after identification of the plant species. Nine dry plant specimens from nine plant species were obtained at Thein-gyi market in Yangon. Only *Andrographis paniculata* overlapped in both the fresh (stem and twigs with leaves) and dry (leaf and stem) samples.

Fresh plant specimens (15–30 g) were extracted with 40 ml of 70% ethanol for two weeks. Dry plant specimens (10–20 g), except the powder of *Brucea javanica* fruits, were also cut into small pieces. These dry samples were extracted with 40 ml of 70% methanol for 7 days at room temperature. The choice for use of ethanol for fresh sample extraction was due to the availability and low toxicity at the time of collecting plant samples. We used methanol for dry sample extraction because methanol was scored slightly higher than ethanol for the screening of antimicrobial components from plants [5]. The extracts were passed through a filter paper (Advantec Toyo Kaisha, Ltd., Tokyo, Japan) and concentrated in a rotary evaporator at 37°C, yielding dried crude extracts in the range of 0.7–28.0% weight of the starting

* CORRESPONDENCE TO: KATAKURA, K., Laboratory of Parasitology, Department of Disease Control, Graduate School of Veterinary Medicine, Hokkaido University, Kita 18, Nishi 9, Kita-ku, Sapporo 060–0818, Japan.
e-mail: kenkata@vetmed.hokudai.ac.jp

Table 1. *In vitro* antitrypanosomal and cytotoxic activities of crude plant extracts

Scientific name (family name)	Parts	% yield of extracts	IC_{50} ($\mu g/ml$) Antitrypanosomal *T. evansi*	Cytotoxicity MRC-5	SI	Traditional uses
Fresh Sample						
Adhatoda vasica Nees. (Acanthaceae)	L	4.8	458.1 ± 189.1	nd		Pulmonary diseases, dry cough
Ageratum conyzoides Linn. (Compositae)	L	2.9	440.6 ± 75.3	nd		Antibacterial
Alpinia officinarum Hance. (Zingiberaceae)	R	5.4	242.2 ± 20.5	nd		Anti-diuretics, aches etc.
Alstonia scholaris R. Br. (Apocyanaceae)	L	1.0	391.7 ± 5.8	nd		Antiseptic, amoebic dysentery
Andrographis paniculata Nees. (Acanthaceae)	STL	1.1	467.4 ± 8.8	nd		Malaria, antipyretic, tonic
Artemesia annua Linn. (Compositae)	L	4.3	316.2 ± 99.4	nd		Malaria
Artemesia annua	Fl	0.8	326.9 ± 47.3	nd		Malaria
Artemesia vulgaris Linn. (Compositae)	LS	16.9	196.9 ± 112.5	nd		Malaria
Asparagus racemosus Willd. (Liliaceae)	R	14.2	325.9 ± 125.6	nd		Diarrhoea, fever, blood tonic
Azadirachta indica (Meliaceae)	L	7.9	167.8 ± 12.5	nd		Diabetes, malaria, skin diseases
Barleria prionitis Linn. (Acanthaceae)	L	4.4	>1000	nd		Diuretic, oedema, pile
Barleria prionitis	L	4.2	252.4 ± 23.9	nd		
Blumea balsamifera DC. (Compositae)	L	2.0	429.5 ± 19.4	nd		Gastric disease, arthritis
Crinum latifolium Linn. (Amaryllidaceae)	L	1.9	443.1 ± 103.9	nd		Dysentry, diarrhoea
Crinum pratense Herb. (Amaryllidaceae)	L	2.3	251.8 ± 72.1	nd		Gonorrhoea, arthritis, dilatation of pupil
Crinum sp.	L	2.7	400.1 ± 51.6	nd		Malaria, dysentery
Curcuma comosa (Zingiberaceae)	Rh	3.6	236.9 ± 6.6	nd		
Elettaria cardamomum Maton. (Zingiberaceae)	L	3.1	157.9 ± 15.8	nd		Dysentery, malaria and diarrhoea
Eucalyptus globulus Labill. (Myrtaceae)	L	0.7	51.1 ± 1.5	622.95 ± 299.7	12.2	Malaria
Euonymus kachinensis (Celastraceae)	L	3.8	232.2 ± 62.2	nd		Relief poisons, sore, antimicrobial
Eupatorium odoratum Linn. (Compositae)	L	9.4	414.7 ± 89.8	nd		Antiseptic, anti tumor
Euphorbia hirta Linn. (Euphorbiaceae)	L	3.1	118.7 ± 7.1	nd		Antimicrobial
Euphorbia longana (Euphorbiaceae)	LFl	5.1	280.3 ± 69.2	nd		Diarrhoea
Holarrhena antidysenterica Wall. (Apocynaceae)	L	1.7	180.6 ± 54.8	nd		Amoebic dysentery, diarrhoea, astringent
Hydrocotyle asiatica Linn. (Umbelliferae)	L	5.3	590.9 ± 25.9	nd		Longevity, leprosy
Ichnocarpus frutescens R.Br. (Apocyanaceae)	L	2.4	205.5 ± 86.1	nd		Tonic, effective on the heart, gallbladder
Jatropha podagrica HK. (Euphorbiaceae)	L	3.5	736.5 ± 186.1	nd		Pulmonary and gastrointestinal diseases
Jatropha podagrica	F	3.7	52.3 ± 13.5	652.7 ± 202.9	12.5	
Kalanchoe laciniata DC. (Crassulaceae)	LT	3.1	396.3 ± 46.5	nd		Dysentery, diarrhoea
Mansonia gagei Drummond. (Sterculiaceae)	L	2.9	789.6 ± 80.8	nd		Fever, dysentery
Morinda angustifolia Roxb. (Rubiaceae)	L	3.5	330.3 ± 11.0	nd		Fever, tonic, dysentery, diarrhoea
Ocimum sanctum Linn. (Labiatae)	LFl	1.8	578.0 ± 251.3	nd		Deodorant, headache, cough
Origanum majorana Linn. (Labiatae)	L	1.9	287.6 ± 73.0	nd		Antimicrobial, anti inflammation, diuretic
Orthosiphon aristatus (Blume) Miq. (Labiatae)	L	3.0	495.0 ± 51.1	nd		Diabetes, arthritis, diuretics
Orthosiphon stamineus (Labiatae)	L	2.6	144.7 ± 36.4	628.9 ± 66.8	4.3	Diabetes, arthritis, diuretics
Physalis peruviana Linn. (Solanaceae)	F	5.4	625.1 ± 86.4	nd		Fever
Piper attenuatum Buch. Ham. (Piperaceae)	L	5.5	282.8 ± 141.9	nd		Malaria
Piper attenuatum	F	5.1	469.6 ± 4.1	nd		
Piper nigrum Linn. (Piperaceae)	L	2.5	170.8 ± 49.4	nd		Malaria
Plumbago rosea Linn. (Plumbaginaceae)	L	1.7	554.5 ± 144.7	nd		Dysmenorrhea, amenorrhea
Plumbago rosea	Fl	2.1	156.7 ± 68.8	557.05 ± 269.4	3.6	
Plumbago zeylanica Linn. (Plumbaginaceae)	L	1.7	268.8 ± 0.9	nd		Leucoderma, scabies, anthelmintic
Rhoeo discolor Hance. (Commelinaceae)	L	1.8	75.8 ± 16.0	424.9 ± 160.0	5.6	Dysentry, diarrhoea
Rhoeo discolor	Fl	1.5	135.5 ± 34.0	>1000		
Rhoeo sp.	L	5.8	808.1 ± 16.1	nd		
Rhoeo sp.	Fl	2.1	490.3 ± 77.2	nd		
Sansevieria cylindrica (Liliaceae)	LT	6.2	208.6 ± 29.5	nd		Dysentry, diarrhoea
Sansevieria zeylanica Wild. (Liliaceae)	LT	1.7	255.6 ± 56.9	nd		Anti venom
Sansevieria zeylanica	L	4.8	400.8 ± 116.4	nd		
Saxifraga virginiensis (Saxifragaceae)	LS	1.8	255.6 ± 27.5	nd		Diuretic, oedema,
Talinum patens L. Wild. (Portulacaceae)	L	1.6	244.6 ± 128.2	nd		Fever, dysentery
Zingiber officinale Rosc. (Zingiberaceae)	L	2.5	305.2 ± 141.8	nd		Asthma, hiccough, cholera, earache
Zingiber officinale	R	2.4	358.6 ± 208.6	nd		
Zizyphus rugosa Lank. (Rhamnaceae)	F	11.8	373.8 ± 145.7	nd		Diarrhoea, tachycardia, skin infection
Zizyphus rugosa	S	0.7	257.6 ± 56.8	nd		

Table 1. *In vitro* antitrypanosomal and cytotoxic activities of crude plant extracts (continued)

Scientific name (family name)	Parts	% yield of extracts	IC_{50} (μg/ml) Antitrypanosomal *T. evansi*	Cytotoxicity MRC-5	SI	Traditional uses
Dry Sample						
From Pathein						
Crataeva religiosa Forst. (Capparidaceae)	LS	4.0	107.1 ± 11.6	691 ± 489.3	6.4	Tumour, as tonic agent, urinary disorders
Eichomia crassipes (Pontederiaceae)	LS	4.2	157.8 ± 47.6	nd		Malaria, fever
Oldenlandia diffusa Willd. (Rubiaceae)	LS	10.0	504.8 ± 21.7	nd		Toothache, haemoptysis, menorrhagia
Phyllanthus niruri Linn. (Euphorbiaceae)	LS	5.9	336.9 ± 53.5	nd		Fever, dysentery
Phyllanthus simplex Retz. (Euphorbiaceae)	LS	2.2	96.1 ± 34.6	98.8 ± 26.0	1.0	Fever, dysentery
Vernonia cenerea Less. (Compositae)	LS	11.5	789.8 ± 2.6	nd		Fever
Vitex arborea Desf. (Verbenaceae)	LS	10.4	48.6 ± 10.9	735.15 ± 374.5	15.1	Fever
From Yangon						
Andrographis sp.	LS	28.0	616.2 ± 0.1	nd		Malaria, antipyretic, tonic
Andrographis paniculata	LS	19.6	54.7 ± 33.1	55.1 ± 20.0	1.0	
Brucea javanica (L.) Merr. (Simaroubaceae)	F	12.5	27.2 ± 7.9	309.15 ± 1.6	11.4	Dysentery, tumor, malaria
Cinnamomum tamala F. Nees. (Lauraceae)	B	17.0	445.9 ± 75.5	nd		Dysentery, antiseptic
Combretum acuminatum (Combretaceae)	Rh	14.0	90.7 ± 11.6	853.15 ± 39.3	9.4	Malaria, dysentery
Gentiana kurroo Royle. (Gentianaceae)	R	10.0	155.3 ± 80.1	nd		To promote digestion, urinary disorders
Tacca pinnatifida Forst. (Taccaceae)	R	4.7	208.4 ± 153.5	nd		Fever
Vitis repens Wight & Arn. (Vitaceae)	RB	2.3	8.6 ± 1.5	209.9 ± 125.5	24.4	Ulcers, hepatitis and jaundice, tumor
Withania somnifera Dunal. (Solanaceae)	SB	4.0	353.2 ± 174.8	nd		Inflammation, diuretic, aphradisiac
Reference drug						
Diminazene aceturate			0.01140 ± 0.001	>1000		

Plant part: L, leaf; R, root; STL, stem and twigs with leaves; F, fruit; Fl, flower; LFl, leaf and flower; LS, leaf and stem; LT, leaf and twig; Rh, rhizomes; RB, rootbark; SB, stembark. nd, not determined.

materials (Table 1). The extracts were dissolved in DMSO and diluted with HMI-9 medium [2] with 0.5% DMSO before use.

Antitrypanosomal activity test was performed in 96-well microtiter plates [2]. Trypomastigotes of bloodstream-form of *Trypanosoma evansi* (H3 strain, isolated from deer in Thailand) were used in this study. Each well contained plant extracts (1.9–1,000 μg/m*l*) and 5×10^4 parasites/m*l* in 100 μ*l* of HMI-9 medium. Diminazene aceturate (Sigma, St. Louis, MO, U.S.A.) was used as a standard trypanocidal drug. Plates were incubated at 37°C in 5% CO_2 in air for 72 hr. Six hours before the end of incubation, 10 μ*l* of Alamar Blue® (TREK Diagnostic Systems, Cleveland, OH, U.S.A.) was added to the cultures, and absorbance at 570 and 600 nm was measured using a plate reader (SpectraMax M5-H, Molecular Devices, Sunnyvale, CA, U.S.A.). IC_{50} (inhibitory concentration, 50%) value was calculated by computerized probit analysis. All tests were performed twice or three times, with each plant extract concentration in triplicate. Cytotoxicity assay against MRC-5 cells (human diploid lung fibroblast cell line, purchased from RIKEN Cell Bank, Tsukuba, Japan) was similarly carried out in 96-well culture plates containing a concentration of 2.5×10^4 cells/m*l* and plant extracts (concentrations of 3.9–1,000 μg/m*l*) in 100 μ*l* of MEM medium (SAFC Biosciences, Lenexa, KS, U.S.A.) supplemented with 3% HEPES (Sigma) and 10% heat inactivated FBS (fetal bovine serum, Gibco, Carlsbad, CA, U.S.A.). After 6 days incubation at 37°C in 5% CO_2 in air, 10 μ*l* Alamar Blue® was added to each well for 6 hr, followed by colorimetric readings, and IC_{50} values were calculated as described above. The selectivity index (SI) was determined by dividing the IC_{50} value for MRC-5 cells by the IC_{50} value for trypanosomes.

The plant species name, plant part used, yield of extract, antitrypanosomal activity, cytotoxicity, SI value and traditional use of 71 plant materials from 60 plant species collected in Myanmar are summarized in Table 1. When IC_{50} values of plant extracts against *T. evansi* were <100 μg/m*l*, cytotoxicity tests against MRC-5 cells were performed. Additionally, some other extracts showing IC_{50} values of 100–200 μg/m*l* were also examined for their cytotoxic activities. As far as we know, except for *Brucea javanica, Andrographis paniculata* and *Plumbago zeylanica*, these plant species were examined for their antiprotozoal activities for the first time. Antiprotozoal activities of medicinal plant crude extracts were classified into four categories, highly active ($IC_{50} \leq 10$ μg/m*l*), active ($IC_{50} > 10 \leq 50$ μg/m*l*), moderately active ($IC_{50} > 50 \leq 100$ μg/m*l*, and non-active ($IC_{50} > 100$ μg/m*l*) [13]. When plant extracts showed SI≥10, these samples are considered to have good selectivity and will be considered for further bio-guided fractionation. According to these criteria, the dry plant extract from rootbark of *Vitis repens* Wight & Arn. (Vitaceae) showed high activity against *T. evansi* (IC_{50}=8.6 μg/m*l*) with good selectivity (SI=24.4). This plant species has been used for the treatment of ulcers, hepatitis/jaundice, and hypertension in Myanmar. The genus Vitis commonly contains various oligomers of resveratrol, such as vitisinols A–D, (+)-σ-viniferin, (–) viniferal, ampelopsin C, miyabenol A, (+)-vitisin A, and (+)-vitisin C [8]. These compounds are of great

interest in further investigation for the antiprotozoal activities.

Brucea javanica (L.) Merr. is widely distributed throughout Asia, where the fruits have been used for various ailments, including cancer, amoebic dysentery, and malaria. Quassinoids isolated from this plant had inhibitory activity against not only *Plasmodium falciparum* [12] but also *Babesia gibsoni in vitro* [16] and *in vivo* [11] as well as against *T. evansi in vitro* [2]. In this study, crude extract from the fruits of *B. javanica* showed the second strongest activity against *T. evansi* (IC_{50}=27.2 ± 7.9 μg/m*l*) and good selectivity (SI=11.4), confirming the previous studies. Further studies are required whether these extracts and quassinoids are also effective against *T. brucei* subspecies.

Vitex arborea Desf. (Verbenaceae) is a small to medium-sized evergreen tree distributed in Asia. In Myanmar, this plant is used for the treatment of fever and diarrhea. The methanol extract from leaf/stem of *Vitex arborea* showed IC_{50} of 48.6 ± 10.9 μg/m*l* and SI of 15.1, but there are no reports of isolated compounds from this plant species. *Jatropha podagrica* (Euphorbiaceae) is a shrub commonly found in Africa, Asia, and Latin America. The major constituents of *Jatropha* species are diterpenoids, which have shown antibacterial activity [1] as well as leishmanicidal and trypanocidal activity [15]. Recently, it has been reported that one xanthone isolated from the roots of *Andrographis paniculata* showed good *in vitro* activity (IC_{50}=4.6 μg/m*l*) against *T. brucei* brucei [4]. The methanol extract from the leaves and stem of this plant species showed IC_{50} value of 54.7 ± 33.1 μg/m*l*, but selectivity index was very low (SI=1) in this study.

In conclusion, the present study revealed that some medicinal plants in Myanmar may offer a potential use for the treatment of *Trypanosoma evansi* infection. Further studies including determination and purification of active compounds in these most promising plant extracts will be carried out.

ACKNOWLEDGMENT(S). We thank Mr. Maung Maung Nyunt, Dr. Aung Gyi, Dr. Myint Thein and all staffs of Livestock Breeding and Veterinary Department and of the University of Veterinary Science, Myanmar, and Mr. Hla Myint of Department of Traditional Medicinal, Ministry of Health, Myanmar and Dr. Kyaw Kyaw Swe for assistance in the collection and identification of plant samples. We also wish to thank Miss E. Tanaka of Hokkaido University for cytotoxic assay. This work was supported in part by the Global COE program, "Establishment of International Collaboration Centers for Zoonosis Control" from MEXT, Japan.

REFERENCES

1. Aiyelaagbe, O. O., Adesogan, K., Ekundayo, O. and Gloer, J. B. 2007. Antibacterial diterpenoids from *Jatropha podagrica* Hook. *Phytochemistry* **68**: 2420–2425.
2. Bawm, S., Matsuura, H., Elkhateeb, A., Nabeta, K., Subeki, Nonaka, N., Oku, Y. and Katakura, K. 2008. *In vitro* antitrypanosomal activities of quassinoid compounds from the fruits of a medicinal plant, *Brucea javanica*. *Vet. Parasitol.* **158**: 288–294.
3. Brun, R., Hecker, H. and Lun, Z.-R. 1998. *Trypanosoma evansi* and *T. equiperdum*: distribution, biology, treatment and phylogenetic relationship (a review). *Vet. Parasitol.* **79**: 95–107.
4. Dua, V. K., Verma, G. and Dash, A. P. 2009. *In vitro* antiprotozoal activity of some xanthones isolated from the roots of *Andrographis paniculata*. *Phytother. Res.* **23**: 126–128.
5. Eloff, J. N. 1998. Which extractant should be used for the screening and isolation of antimicrobial components from plants? *J. Ethnopharmacol.* **60**: 1–8.
6. Hoet, S., Opperdoes, F., Brun, R. and Quetin-Leclercq, J. 2004. Natural products active against African trypanosomes: a step towards new drugs. *Nat. Prod. Rep.* **21**: 353–364.
7. Kibona, S. N., Matemba, L., Kaboya, J. S. and Lubega, G. W. 2006. Drug-resistance of *Trypanosoma b. rhodesiense* isolates from Tanzania. *Trop. Med. Int. Health* **11**: 144–155.
8. Li, W. W., Li, B. G. and Chen, Y. Z. 1998. Flexuosol A, a new tetrastilbene from *Vitis flexuosa*. *J. Nat. Prod.* **61**: 646–647.
9. Luckins, A. G. 1988. *Trypanosoma evansi* in Asia. *Parasitol. Today* **4**: 137–142.
10. Matovu, E., Seebeck, T., Enyaru, J. and Kamisnky, R. 2001. Drug resistance in *T. brucei* spp., the causative agents of sleeping sickness in man and nagana in cattle. *Microbes Infect.* **3**: 763–770.
11. Nakao, R., Mizukami, C., Kawamura, Y., Subeki, Bawm, S., Yamasaki, M., Maede, Y., Matsuura, H., Nabeta, K., Nonaka, N., Oku, Y. and Katakura, K. 2009. Evaluation of efficacy of bruceine A, a natural quassinoid compound extracted from a medicinal plant, *Brucea javanica*, for canine babesiasis. *J. Vet. Med. Sci.* **71**: 33–41.
12. O'Neill, M. J., Bray, D. H., Boardman, P., Phillipson, J. D., Warhurst, D. C., Peters, W. and Suffness, M. 1986. Plants as sources of antimalarial drugs: *in vitro* antimalarial activities of some quassinoids. *Antimicrob. Agents Chemother.* **30**: 101–104.
13. Osorio, E., Arango, G. J., Jiménez, N., Alzate, F., Ruiz, G., Gutiérrez, D., Paco, M. A., Giménez, A. and Robledo, S. 2007. Antiprotozoal and cytotoxic activities *in vitro* of Colombian Annonaceae. *J. Ethnopharmacol.* **111**: 630–635.
14. Soe, K. and Ngwe, T. M. 2004. Medicinal Plants of Myanmar: Identification and Uses of Some 100 Commonly Used Species Series (1), Forest Resource Environment Development and Conservation Association, Yangon.
15. Schmeda-Hirschmann, G., Razmilic, I., Sauvain, M., Moretti, C., Muñoz, V., Ruiz, E., Balanza, E. and Fournet, A. 1996. Antiprotozoal activity of jatrogrossidione from *Jatropha grossidentata* and jatrophone from *Jatropha isabelli*. *Phytother. Res.* **10**: 375–378.
16. Subeki, Matsuura, H., Takahashi, K., Nabeta, K., Yamasaki, M., Maede, Y. and Katakura, K. 2007. Screening of Indonesian medicinal plant extracts for anti-babesial activity and isolation of new quassinoids from *Brucea javanica*. *J. Nat. Prod.* **70:** 1654–1657.

Parasitology International 59 (2010) 647–652

Contents lists available at ScienceDirect

Parasitology International

journal homepage: www.elsevier.com/locate/parint

Short communication

Gene silencing in *Echinococcus multilocularis* protoscoleces using RNA interference

Chiaki Mizukami [a], Markus Spiliotis [b], Bruno Gottstein [b], Kinpei Yagi [c], Ken Katakura [a], Yuzaburo Oku [a,*]

[a] Laboratory of Parasitology, Department of Disease Control, Graduate School of Veterinary Medicine, Hokkaido University, Sapporo 060-0818, Japan
[b] Institute of Parasitology, University of Berne, Länggass-Strasse 122, CH-3001 Berne, Switzerland
[c] Hokkaido Institute of Public Health, Sapporo 060-0819, Japan

ARTICLE INFO

Article history:
Received 15 April 2010
Received in revised form 23 August 2010
Accepted 24 August 2010
Available online 9 September 2010

Keywords:
Cestode
Echinococcus multilocularis
Protoscolex
RNAi
siRNA

ABSTRACT

We investigated the potential of gene silencing in *Echinococcus multilocularis* protoscoleces using RNA interference (RNAi). For the introduction of siRNA, soaking and electroporation were first examined for their effects on the viability of protoscoleces and their efficacy for siRNA introduction. Consequently, electroporation using 100 V and 800 μF showed the optimal results. This electroporation procedure was then evaluated for its ability to induce RNAi in protoscoleces using siRNAs targeting the *14-3-3* and *elp* genes. It was found that the levels of *14-3-3* and *elp* mRNA in *14-3-3* siRNA- and *elp* siRNA-treated protoscoleces were reduced to 21.8 ± 2.6 and 35.5 ± 0.4% of those of the untreated control by day 3, respectively. Moreover, the target proteins significantly decreased in the siRNA-treated samples by day 15. In the analysis of viability, the untreated control, electroporation control, *14-3-3* siRNA-treated, and *elp* siRNA-treated samples displayed 98.4 ± 1.4, 83.0 ± 2.5, 58.0 ± 23.0, and 55.1 ± 14.6% viability, respectively, on day 15. In conclusion, we successfully demonstrated that RNAi mediated the knock-down of target gene expression in *E. multilocularis* protoscoleces at both the transcriptional and translational levels.

Larval stage infection with *Echinococcus multilocularis* causes alveolar echinococcosis, one of the most lethal helminthic infections in humans, demonstrating a greater than 90% fatality rate in untreated patients [1]. Recently, *E. multilocularis* has emerged as a model experimental research system given its interesting characteristics, including its continuous active proliferation and underlying molecular mechanisms of host-parasite interactions [2], in addition to the availability of well-developed *in vivo* maintenance methods using mice and gerbils and *in vitro* cultivation systems [3]. Studies in this organism are also facilitated by available genetic information, such as cDNA sequences and genomic databases (i.e., http://fullmal.hgc.jp/em/; http://www.sanger.ac.uk/Projects/Echinococcus/), long-term *in vitro* cultivation techniques of primary cells, and the ability to transiently transfect cells using plasmids and *Listeria monocytogenes* [4]. However, no methods have been established so far, that allow to knock-out or knock-down the expression of specific genes in *E. multilocularis*.

In this study, we investigated the potential of gene silencing in *E. multilocularis* protoscoleces using RNA interference (RNAi). RNAi is a mechanism in which the degradation of mRNA is induced by complementary short interfering RNA (siRNA) through intracellular mechanisms that have been widely conserved during evolution; as a consequence of these events, gene expression can be effectively suppressed [5]. An advantage of RNAi is its ability to provide information regarding gene function in a relatively quick and easy manner [6], and represents a promising technique for gene function analysis that has been successfully applied in numerous organisms to date. In the phylum Platyhelminthes, RNAi was achieved via soaking and electroporation processes for the introduction of siRNA in schistosomules [7–9], *Fasciola hepatica* [10], and planaria [11]. Among cestodes, Pierson et al. recently reported successful RNAi in adult worms of *Moniezia expansa* using dsRNA [12]. It was therefore expected that this technique could also be applied to *E. multilocularis*, which would greatly facilitate the investigation of gene function and identification of essential gene products of this deadly parasite, and should help to provide important knowledge for the control of echinococcosis.

The protoscoleces of *E. multilocularis* can be isolated in large quantities from fertile metacestode tissues obtained from laboratory animals, and can subsequently be easily maintained *in vitro* for several weeks. Interestingly, protoscoleces are able to develop into either adults or larval vesicles [13]. Thus, protoscoleces represent an attractive research material to study the mechanisms and factors involved in several developmental stages of this parasite.

The *14-3-3* (GenBank accession no. U63643) and *elp* (AJ012663) genes of *E. multilocularis*, which encode for 14-3-3 and antigen II/3, respectively, served as the model target genes in this study. The 14-3-3 proteins constitute a family of conserved ubiquitous eukaryotic proteins that are involved in a number of important cellular processes, including signal transduction, cell-cycle control, apoptosis, stress response, and malignant transformation [14]. In *E. multilocularis*, one 14-3-3 isoform has been published so far which is similar to the zeta isoform in higher eukaryotes and is highly expressed at the metacestode stage and mainly localizes to the germinal layer of cysts

* Corresponding author. Tel./fax: +81 11 706 5196.
E-mail address: oku@vetmed.hokudai.ac.jp (Y. Oku).

1383-5769/$ – see front matter © 2010 Elsevier Ireland Ltd. All rights reserved.
doi:10.1016/j.parint.2010.08.010

and the apical structures in both invaginated and evaginated protoscoleces [15]. The protein encoded by the *elp* gene, which has been referred to as antigen II/3, Em10, or Em18, is expressed in both *E. multilocularis* adult and metacestode stages and has been used as an important diagnostic antigen [16]. Antigen II/3 shares homology with the mammalian ezrin, radixin, and moesin (ERM) protein family [17] that is involved in several key processes related to cellular architecture maintenance, including cell–cell adhesion, membrane trafficking, microvillus formation, transmembrane signaling, and cell division [18]. In *E. multilocularis*, antigen II/3 localizes within the germinal layer and parenchymal cells of protoscoleces and on the surface of calcareous corpuscles (Fig. 1 of [19]). Matsumoto et al. reported that the combination of 14-3-3 and antigen II/3 expression could be used as a molecular marker of viability and growth activity in *E. multilocularis* [20].

All experiments in this study were performed using protoscoleces isolated from the *E. multilocularis* Nemuro strain maintained at the Hokkaido Institute of Public Health (Sapporo, Japan). To isolate protoscoleces, larval cyst masses isolated from cotton rats (*Sigmodon hispidus*) were minced, passed through a sieve (100-μm mesh size), and then washed repeatedly with 0.85% physiological saline until host materials were thoroughly removed. The protoscoleces were then treated with 0.5% hydrochloric acid and 0.5% pepsin dissolved in 0.85% physiological saline for 30 min to digest any remaining host tissue (this treatment can be a stimulus for differentiation to adults), and were subsequently cultured in CMRL1066 medium (Gibco) supplemented with 10% fetal calf serum (Gibco), 200 U/ml penicillin G, and 200 μg/ml streptomycin (Gibco) in culture flasks for 1–2 days at 37 °C in the presence of 100% N_2.

For the RNAi experiments, we attempted to select suitable conditions in which protoscoleces could maintain high viability. The negative control RNAi experiments were performed using fluorescently labeled (FAM-labeled negative control #1 siRNA, Ambion) and negative control (Silencer negative control #1 siRNA, Ambion) siRNAs. The sequence of negative control #1 siRNA was unknown, as it is proprietary information of Ambion; however, the company states that the siRNA does not specifically target any human, mouse, or rat gene. To determine the suitable conditions for siRNA introduction, soaking and electroporation were tested without siRNA. Soaking was performed with 1–30 μl transfection reagent (NeoFX, Ambion) in 100 μl culture medium and electroporation was performed at 100–400 V (100-V intervals) and 100–1,000 μF (100-μF intervals) to examine their effects on the viability of the protoscoleces. The results of these tests revealed that protoscoleces exhibited greater than 80% viability 3 days after either soaking with 0–10 μl transfection reagent or electroporation at 100 V with 100–800 μF or 200 V with 100 μF.

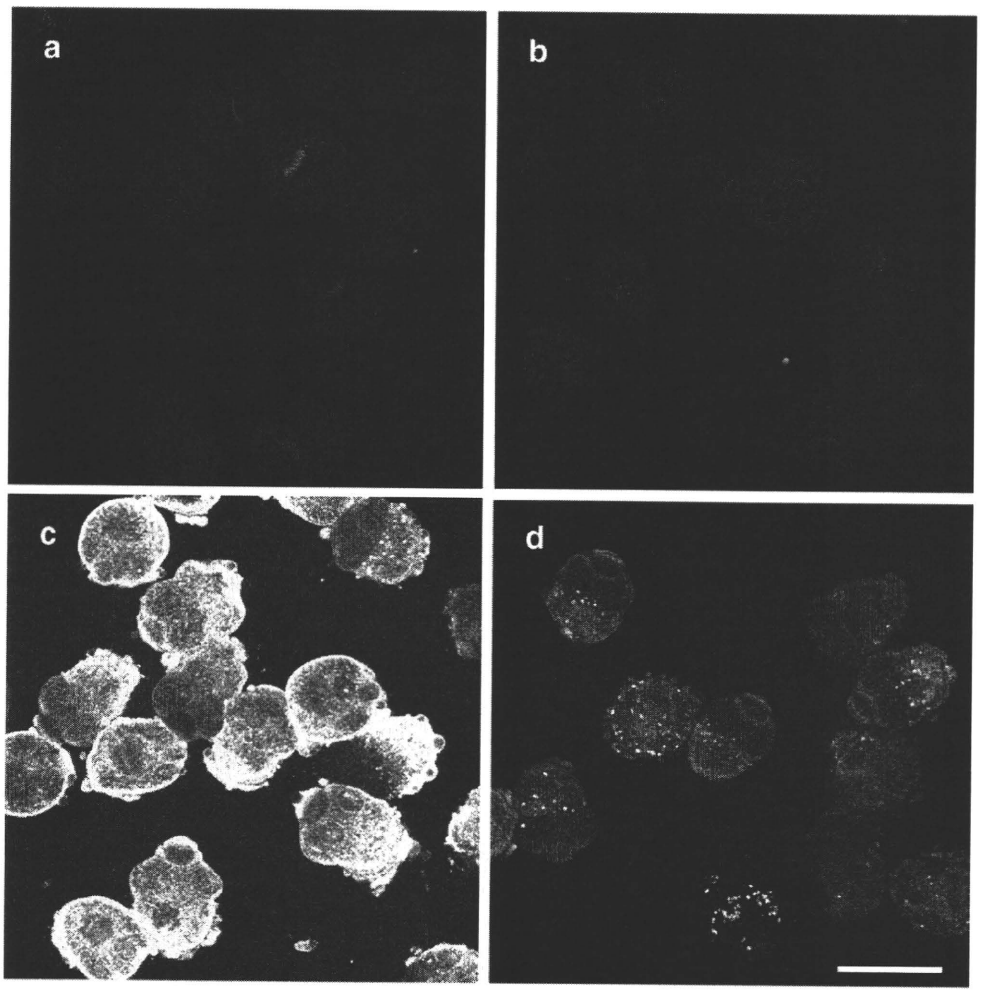

Fig. 1. Localization of fluorescently labeled siRNA following soaking or electroporation. Parasites untreated (a) or treated with fluorescently labeled siRNA via soaking in transfection reagent (b) or electroporation (c and d) were observed by confocal microscopy. At 30 min after electroporation, strong fluorescence was detected in the parasites (c). Diminished fluorescence and several bright spots were observed in protoscoleces 2 h after electroporation (d). No fluorescence was detected in the parasites of the untreated control (a) or parasites treated by soaking (b) 30 min after treatment. The scale bar indicates 200 μm.

The three promising candidate conditions, soaking with 10 μl transfection reagent, and electroporation with 100 V–800 μF and 200 V–100 μF, were tested for their efficacy of siRNA introduction using fluorescently labeled siRNA. For soaking, 100 μl culture medium containing approximately 2,000 protoscoleces was placed in a 24-well plate, and the fluorescently labeled siRNA (5 μM final concentration) alone or with 10 μl transfection reagent (NeoFX, Ambion) was then added to each well. The parasites were incubated at 37 °C in the presence of 5% CO_2 in the dark. For electroporation, 100 μl electroporation buffer (Ambion) containing approximately 2,000 protoscoleces was placed in a 4-mm cuvette, and the fluorescently labeled siRNA was added to give a final concentration of 5 μM. Electroporation was performed at 100 V–800 μF or 200 V–100 μF using an exponential decay pulse (Gene Pulser II, Bio-Rad). After incubation at 37 °C for 10 min, the buffer containing protoscoleces was transferred into 1 ml culture medium, which was then further incubated at 37 °C in 24-well plates in the presence of 5% CO_2 in the dark. At 30 min and 2 h after treatment, the parasites were washed with PBS and viewed under a fluorescent microscope (FV500, Olympus) to evaluate the efficacy of the three treatment conditions.

As expected, fluorescence was not detected in the untreated parasites (Fig. 1a). Surprisingly, fluorescence was also undetectable in the parasites treated by soaking with (Fig. 1b) or without transfection reagent (data not shown). We had previously hypothesized that the tegument, the surface syncytial structure that covers the entire body of the protoscolex and is involved in the active transport of extrasomatic low molecular weight nutrients [21], would be suitable for the absorption of siRNA. However, soaking proved to be unsuccessful for the introduction of siRNA into the parasites. In contrast, in the parasites treated by electroporation at 100 V–800 μF, strong fluorescence was detected 30 min after treatment (Fig. 1c), although the fluorescence decreased 2 h after treatment (Fig. 1d). Electroporation at 200 V–100 μF showed a very similar result to the 100 V–800 μF conditions (data not shown). The reason for the loss of fluorescence at 2 h after treatment is unknown. Krautz-Peterson et al. reported successful gene suppression in schistosomules using RNAi, although a similar reduction in fluorescence was observed in the method they used [9]. According to our present results, the electroporation condition of 100 V–800 μF was selected for the introduction of siRNA into protoscoleces in the subsequent experiments.

We next examined the efficacy of RNAi with the selected electroporation conditions. The respective target sequences were determined using the BLOCK-iT RNAi Designer software (https://rnaidesigner.invitrogen.com/rnaiexpress/), and the resulting 23 nt designed siRNA duplexes were obtained from Sigma-Aldrich at a concentration of 100 μM. The sequence of the siRNA targeting *14-3-3 zeta* was 5'-GCU CGU CGU UCA UCG UGG AGA AU-3' without a overhang, and that targeting *elp* was 5'-AAC CUU UCU AAG ACU GGA UAA GA-3' without a overhang. To analyze the effects of siRNA introduction into *E. multilocularis*, four sample groups of protoscoleces were prepared: untreated controls, electroporation controls, *14-3-3* siRNA-treated samples, and *elp* siRNA-treated samples. One hundred microliters of electroporation buffer (Ambion) containing approximately 2,000 protoscoleces was placed in a 4-mm cuvette for each sample. siRNA targeting *14-3-3* or *elp* at a final concentration of 3 μM was added to each cuvette of the 14-3-3 or *elp* siRNA-treated sample group, respectively. The negative control siRNA (Silencer negative control #1 siRNA, Ambion) was added to all of the electroporation controls at a final concentrations of 3 μM. Electroporation was then performed at 100 V–800 μF using an exponential decay pulse (Gene Pulser II, Bio-Rad). After incubation at 37 °C for 10 min, the buffer containing protoscoleces was transferred into 1 ml culture medium in the well of a 24-well plate. For the untreated controls, 2,000 protoscoleces were directly transferred from flasks into 1 ml culture medium. All samples were further incubated at 37 °C in the presence of 5% CO_2 in the dark and half of the medium was changed every 3 days. The analyses were performed in triplicate for each group.

The RNAi effects on mRNA levels were evaluated using real-time RT-PCR. For the analyses, total RNA was first extracted from all groups at day 0 and 3 after electroporation using TRIzol reagent (Invitrogen), and cDNA was then synthesized from 200 ng RNA in a total volume of 10 μl using the PrimeScript RT Reagent Kit (Takara) according to the manufacturer's instructions. Real-time PCR was carried out using 2 μl of 1:100 cDNA dilution, SYBR Premix Ex Taq II (Takara) and the following primer sets: *14-3-3 zeta* forward 5'-AAC TTG CTA TCC GTT GC-3', reverse 5'-CAC CTT CTT AAG GTA AAT GTC-3'; *elp* forward 5'-GTG AAG TCT GGT ACT TCG-3', reverse 5'-ATC CAG TCT TAG AAA GGT TG-3'; *actin 2* forward 5'-TCA ATC CTA AAG CCA ATC-3', reverse 5'-CGT ACA ACG ACA GCA C-3' for *emactin2* (XvEMb06047 from our cDNA library, http://fullmal.hgc.jp/em/); *14-3-3 epsilon* forward 5'-ATC TTA ATG ATG AAT CCG CTC CTG- 3', reverse 5'-GTT CAT CGC CCT CAT CCT TG- 3' for *14-3-3 epsilon* (Emmg-5f10.q1k, http://www.sanger.ac.uk/Projects/Echinococcus/). All samples were run in triplicate and underwent 40 amplification cycles at 95 °C for 5 s and 60 °C for 31 s using a StepOne Real-Time PCR System (Applied Biosystems). The amount of each cDNA was then calculated using standard curves and compared to the relative amounts of *emactin2*, an endogenous standard. Each relative amount was subsequently normalized to the untreated control at day 0. Statistical analyses using one-way ANOVA and Tukey's multiple comparison test were then performed.

The results of the real-time RT-PCR analyses revealed that *14-3-3 zeta* mRNA reduced to 21.8 ± 2.6% of the untreated control levels in *14-3-3* siRNA-treated protoscoleces by day 3, which was significantly ($P<0.01$) lower than the levels of the untreated control, electroporation control, and *elp* siRNA-treated samples (Fig. 2a). The levels of *elp* mRNA were also low in *elp* siRNA-treated protoscoleces, decreasing to 35.5 ± 0.4% of the untreated control levels by day 3, whereas the *elp* mRNA levels in the electroporation control and *14-3-3* siRNA-treated samples were 64.6 ± 19 and 57.5 ± 1.7% of the untreated control; however, ANOVA analyses suggested that the differences were not statistically significant (Fig. 2c). No significant reduction was observed in *14-3-3 epsilon* mRNA in any sample (Fig. 2b), even though *14-3-3 epsilon* mRNA contained a sequence which matches 21 of the 23 siRNA bases targeting the 14-3-3 zeta protein. This result suggested that as few as two base differences ensures the specificity of siRNA in *E. multilocularis*. All target mRNAs showed modest reductions in the electroporation controls; however, no statistical differences were observed between the untreated and electroporation controls.

The RNAi effects on protein expression levels were evaluated using western blot analysis. The treated protoscoleces were collected on day 3, 6, 10, and 15 after electroporation and homogenized using a hand homogenizer (23 M-R25, Nippon Genetics). Fifty microliters of radioimmunoprecipitation assay (RIPA) buffer containing 25 mM Tris, 150 mM NaCl, 5 mM EDTA, 1% sodium deoxycholate, 1% Triton X-100, and 0.1% SDS (pH 7.5) was added, and the specimens were treated by repeated freezing and thawing. Fifty microliters of 2× SDS sample buffer (100 mM Tris, 4% SDS, 12% 2-mercaptoethanol, 20% glycerol, and a few drops of bromphenol blue (BPB) solution (pH 6.8)) was added to the samples, which were then heated at 90 °C for 10 min and centrifuged at 20,000×g for 10 min. Extracted proteins were size separated on 12% acrylamide gels and transferred to polyvinylidene fluoride (PVDF) membranes. Detection of the specific proteins was performed using rabbit anti-14-3-3 [22], rabbit anti-antigen II/3 [20], and rabbit anti-actin (anti-beta-actin (NT), AnaSpec) antibodies as the primary antibodies, and goat anti-rabbit antibody (anti-rabbit IgG AP conjugate, Promega) as the secondary antibody. In the western blot obtained under reducing conditions, we identified a specific 27-kDa protein with the anti-14-3-3 antibody, 65-kDa and 52-kDa proteins with the anti-antigen II/3 antibody, and a 42-kDa protein with the anti-actin antibody. The detection of two II/3 protein bands has been reported previously by Felleisen & Gottstein, who speculated that

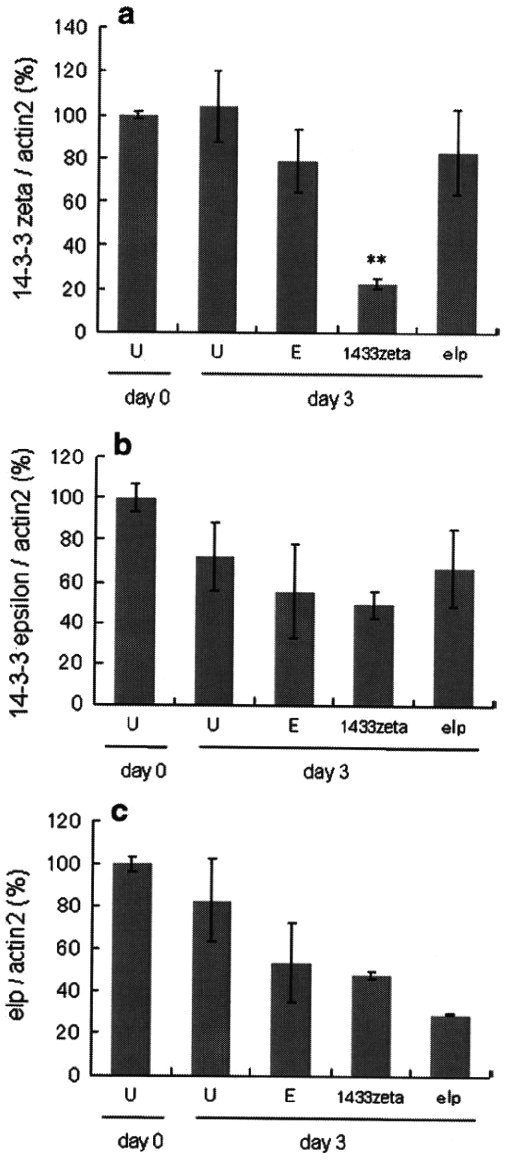

Fig. 2. RNAi effects on mRNA levels in *E. multilocularis* protoscoleces. Relative amounts of each mRNA were detected using real-time RT-PCR. *14-3-3 zeta* mRNA significantly reduced to 21.8 ± 2.6% of the untreated control levels in *14-3-3* siRNA-treated protoscoleces by day 3 (a). No significant reduction was observed in *14-3-3 epsilon* mRNA in any sample (b). The *elp* mRNA levels were lowered in *elp* siRNA-treated protoscoleces, reducing to 35.5 ± 0.4% of the untreated control by day 3. The electroporation control and *14-3-3* siRNA-treated samples showed *elp* mRNA levels of 64.6 ± 19 and 57.5 ± 1.7%, respectively, of the untreated controls. However, ANOVA analyses suggested that the differences between the siRNA-treated samples were not statistically significant (c). U: untreated control; E: electroporation control. Bars represent the standard deviation. $^{**}P<0.01$.

the 52-kDa protein could potentially be a processing or degradation product of the 65-kDa protein [19]. The PVDF membranes were air dried and scanned (Fig. 3a, b), and densitometry analyses were carried out using Photoshop 6.0 (Adobe). The values of the 14-3-3- and II/3-protein blots were normalized to those of actin and then transformed to set the untreated control of each day as 100%. The data were analyzed statistically using one-way ANOVA and Tukey's multiple comparison test. It was revealed that 14-3-3 protein gradually decreased to 41.6 ± 9.7, 39.7 ± 11.7, and 22.1 ± 7.1% of the untreated control levels by day 6, 10, and 15, respectively, in the *14-3-3* siRNA-treated samples. In the electroporation controls, 14-3-3 protein displayed a modest reduction compared to the untreated control from day 6 to 15 (70.0 ± 29.1 (day 6), 64.2 ± 15.0 (day 10), and 72.2 ± 5.2% (day 15) of the untreated control). Statistical analysis indicated that 14-3-3 protein was significantly reduced in siRNA-treated samples by day 15 (Fig. 3c). The densitometry analyses also demonstrated that the II/3-upper protein (65 kDa) levels were reduced to 88.2 ± 33.0, 87.2 ± 6.7, 59.6 ± 4.6, and 68.7 ± 4.6% of the untreated control by day 3, 6, 10, and 15, respectively, in the *elp* siRNA-treated samples. No reduction was observed in electroporation controls. Statistical analysis showed that II/3-upper protein was significantly reduced in the *elp* siRNA-treated samples by day 15 (Fig. 3d). The expression of the II/3-lower protein (52 kDa) was also decreased, with levels of 69.9 ± 5.5, 46.4 ± 5.2, 34.3 ± 2.7, and 26.2 ± 1.8% of untreated control observed by day 3, 6, 10, and 15, respectively, in the *elp* siRNA-treated samples. A modest effect was observed in the electroporation control by day 10 and 15, as the II/3-lower protein decreased to 78.5 ± 29.8 and 62.2 ± 6.0%, respectively, of the untreated control levels. Statistical analysis indicated that II/3-lower protein (52 kDa) was significantly reduced in the siRNA-treated samples on day 6 and 15 (Fig. 3e).

When a comparison was made with the electroporation controls that were set as 100%, the 14-3-3, II/3-upper (65 kDa), and II/3-lower (52 kDa) proteins reduced to 30.6 ± 9.9, 60.8 ± 4.0, and 42.1 ± 3.0%, respectively, in the corresponding siRNA-treated samples by day 15. It is speculated that the anti-14-3-3 antibody likely does not distinguish between the 14-3-3 isoforms, as it detected 14-3-3 isoforms other than what were targeted by the 14-3-3 zeta siRNA, indicating it is highly possible that 14-3-3 zeta itself was reduced to a greater extent than shown in these experiments. The results presented here suggest that RNAi did not uniformly affect the target genes in *E. multilocularis* protoscoleces. In this study, the knock-down of *14-3-3* was the most effective. The observed differences in the efficiency of RNAi on the *14-3-3* and *elp* (antigen II/3) mRNA and resulting protein levels may be due to differences of protein distribution within cells. It was previously reported that 14-3-3 protein mainly localizes in the apical region, pad and adjacent structures, and suckers of protoscoleces [15], whereas antigen II/3 localizes within the germinal layer and in the periphery of individual cell conglomerates inside of protoscoleces [19]. As shown in Fig. 1, it appeared that the amount of siRNA introduced into the surface structures was larger than that found in the internal regions of protoscoleces. It is therefore possible that more siRNA was delivered to cells actively producing 14-3-3 than to those cells producing antigen II/3. In addition to this speculation, the properties and stability of the target mRNAs and proteins may be involved in the difference knock-down efficiencies between the two proteins. The II/3-upper protein (65 kDa) seemed to be less sensitive to both electroporation and siRNA than the lower protein (52 kDa). Although the reason for the difference is unknown, again, the individual properties and stability of the two protein forms may be involved. Unexpectedly, we also observed protein reduction in a few of the electroporation control samples, suggesting that the electroporation treatment could affect the protein expression to a certain degree. It is considered that the reductions were a result of the electroporation procedure itself and were not caused by off-target effects of the negative control siRNA, since it was suggested that a mismatch of two nucleotides could ensure the specificity of siRNA (Fig. 2a and b), and a similar reduction was observed after electroporation without siRNA (data not shown). The differences of the electroporation treatment effects on the protein levels were likely due to differences in localization, stability, or other characteristics of these proteins. In future studies, it may be necessary to consider that observed reductions of target proteins in siRNA-treated samples would include effects by electroporation treatment, in addition to the RNAi effect, and appropriate controls should therefore be included.

Finally, the effects of siRNA introduction by electroporation on the viability of the protoscoleces were evaluated in all samples on day 3, 6, 10, and 15. Viability was calculated by counting the number of living protoscoleces that exhibited a clear appearance and that contained

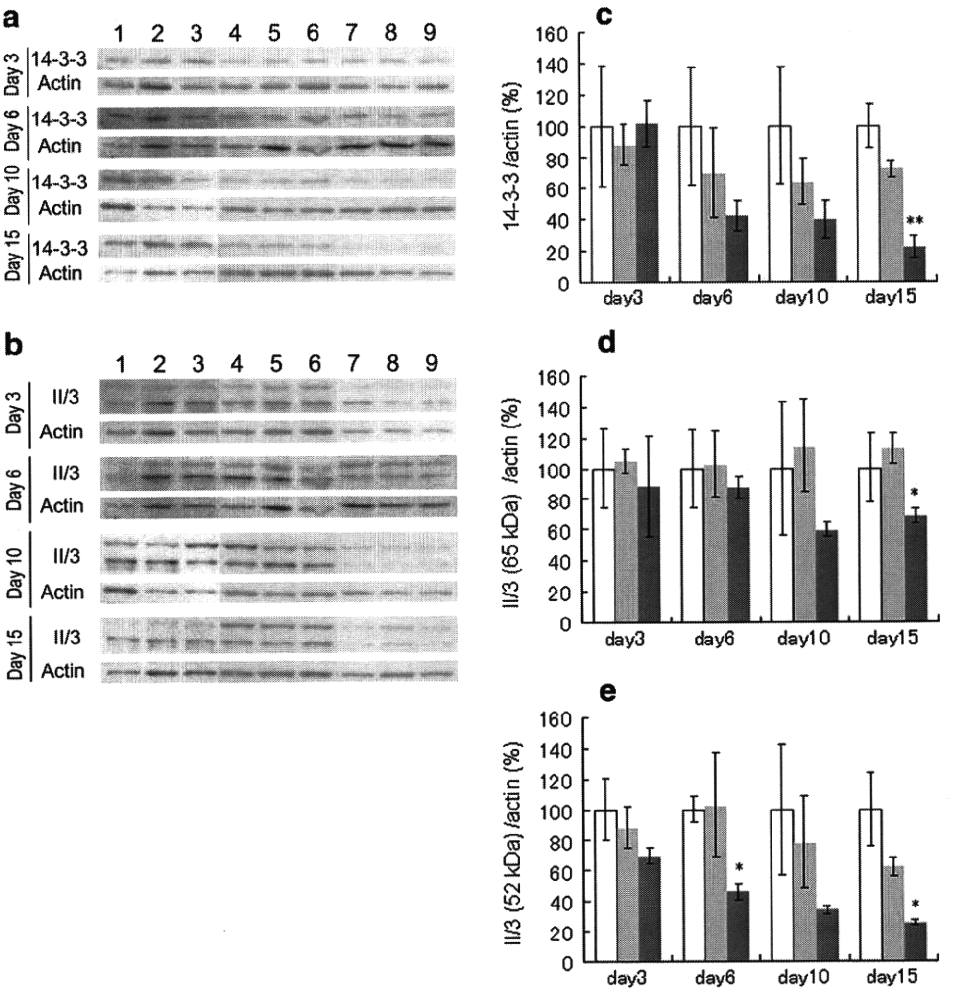

Fig. 3. RNAi effects on protein expression levels in *E. multilocularis* protoscoleces. Detection of 14-3-3, II/3 (*elp*), and actin was performed by western blotting. Untreated control (a and b, lanes 1–3), electroporation control (a and b, lanes 4–6), samples treated with siRNA targeting *14-3-3 zeta* (a, lanes 7–9), samples treated with siRNA targeting *elp* (b, lanes 7–9). The 14-3-3- and II/3-protein blots were evaluated by densitometry analyses. The values were normalized to those of actin and then transformed to set the untreated control levels of each day as 100%. The data were analyzed statistically by using one-way ANOVA and Tukey's multiple comparison test. 14-3-3 protein decreased to 41.6 ± 9.7, 39.7 ± 11.7, and 22.1 ± 7.1% of untreated control levels at day 6, 10, and 15, respectively, in the *14-3-3* siRNA-treated samples. (c). II/3-upper protein was reduced to 88.2 ± 33.0, 87.2 ± 6.7, 59.6 ± 4.6, and 68.7 ± 4.6% of the untreated control by day 3, 6, 10, and 15, respectively, in the *elp* siRNA-treated samples. No reduction was observed in the electroporation controls (d). II/3-lower protein decreased to 69.9 ± 5.5, 46.4 ± 5.2, 34.3 ± 2.7, and 26.2 ± 1.8% of the untreated control by day 3, 6, 10, and 15, respectively, in the *elp* siRNA-treated samples (e). $^{*}P<0.05$, $^{**}P<0.01$.

transparent structures and the number of dead protoscoleces that appeared opaque and demonstrated a rough surface and damaged inner structures. On day 3 and 6, no significant reduction of viability was observed in siRNA-treated samples. By day 10, the untreated control, electroporation control (silencer negative siRNA-treated), *14-3-3* siRNA-treated, and *elp* siRNA-treated samples displayed 94.6 ± 3.4, 86.5 ± 1.4, 80.1 ± 3.0, and 78.4 ± 4.0% viability, respectively, and by day 15, viabilities of 98.4 ± 1.4, 83.0 ± 2.5, 58.0 ± 23.0, and 55.1 ± 14.6%, respectively, were observed. The data of each day were analyzed by one-way ANOVA and Tukey's multiple comparison test, and a significant siRNA effect was found only between the controls (untreated and electroporation controls) and *elp* siRNA-treated samples on day 10. Despite the lack of statistical significance, the observed trend of decreasing viability in *14-3-3* and *elp* siRNA-treated protoscoleces indicates that these two proteins play important roles in essential cellular activities [14,18]. The 14-3-3 zeta protein is consider to have high potential as a vaccine candidate to larval echinococcosis [23], and a DNA vaccine consisting of *TEG-Tsag*, which is a homolog to *elp*, displayed significant levels of protection in a *Taenia crassiceps* murine model of cysticercosis [24].

In morphological observation, several protoscoleces increased in length and others swelled after the 15-day culture in both the control and treated groups. Although the number of swelled protoscoleces increased by a certain degree in samples treated by electroporation (controls and siRNA-treated), no clear difference was found by microscopic observation between the electroporation controls and siRNA-treated protoscoleces.

In conclusion, we demonstrated the potential of gene silencing in *E. multilocularis* protoscoleces using an RNAi method involving electroporation that induced reductions of target mRNA, target protein, and viability in *E. multilocularis* protoscoleces. Despite its successful application, further improvements to this method may be necessary, as it required relatively high concentrations of siRNA (3 or 5 μM), RNAi effects were not observed until several days after siRNA introduction, and the electroporation treatment may cause reductions in the levels of certain proteins. Nevertheless, this method represents a powerful tool for investigating gene function and identifying essential gene products in *E. multilocularis* protoscoleces.

Care of experimental animals

All animal experiments were carried out in accordance with the ethical guidelines of Hokkaido University and Hokkaido Prefecture.

Acknowledgements

We thank Dr. Jun Matsumoto (Nihon University) and Dr. Nariaki Nonaka (University of Miyazaki) for many helpful suggestions regarding the experiments. This study was supported by a Grant-in-Aid for Scientific Research from the Ministry of Education, Culture, Sports, Science and Technology of Japan (Grant no. 20380164), a Grant for Research on New Influenza, Emerging and Re-emerging Infectious Diseases from the Ministry of Health, Labour and Welfare of Japan, and a grant from the Swiss National Science Foundation (grant no. 3100A0-111780).

References

[1] Craig PS, Rogan MT, Allan JC. Detection, screening and community epidemiology of taeniid cestode zoonoses: cystic echinococcosis, alveolar echinococcosis and neurocysticercosis. Adv Parasitol 1996;38:169–250.
[2] Brehm K, Spiliotis M. The influence of host hormones and cytokines on *Echinococcus multilocularis* signalling and development. Parasite 2008;15:286–90.
[3] Brehm K, Spiliotis M. Recent advances in the in vitro cultivation and genetic manipulation of *Echinococcus multilocularis* metacestodes and germinal cells. Exp Parasitol 2008;119:506–15.
[4] Spiliotis M, Lechner S, Tappe D, Scheller C, Krohne G, Brehm K. Transient transfection of *Echinococcus multilocularis* primary cells and complete in vitro regeneration of metacestode vesicles. Int J Parasitol 2008;38:1025–39.
[5] Kurreck J. RNA interference: from basic research to therapeutic applications. Angew Chem Int Ed Engl 2009;48:1378–98.
[6] Cottrell TR, Doering TL. Silence of the strands: RNA interference in eukaryotic pathogens. Trends Microbiol 2003;11:37–43.
[7] Boyle JP, Wu XJ, Shoemaker CB, Yoshino TP. Using RNA interference to manipulate endogenous gene expression in *Schistosoma mansoni* sporocysts. Mol Biochem Parasitol 2003;128:205–15.
[8] Correnti JM, Brindley PJ, Pearce EJ. Long-term suppression of cathepsin B levels by RNA interference retards schistosome growth. Mol Biochem Parasitol 2005;143:209–15.
[9] Krautz-Peterson G, Radwanska M, Ndegwa D, Shoemaker CB, Skelly PJ. Optimizing gene suppression in schistosomes using RNA interference. Mol Biochem Parasitol 2007;153:194–202.
[10] McGonigle L, Mousley A, Marks NJ, Brennan GP, Dalton JP, Spithill TW, et al. The silencing of cysteine proteases in *Fasciola hepatica* newly excysted juveniles using RNA interference reduces gut penetration. Int J Parasitol 2008;38:149–55.
[11] Pineda D, Rossi L, Batistoni R, Salvetti A, Marsal M, Gremigni V, et al. The genetic network of prototypic planarian eye regeneration is Pax6 independent. Development 2002;129:1423–34.
[12] Pierson L, Mousley A, Devine L, Marks NJ, Day TA, Maule AG. RNA interference in a cestode reveals specific silencing of selected highly expressed gene transcripts. Int J Parasitol 2009;40:605–15.
[13] Gottstein B. Molecular and immunological diagnosis of echinococcosis. Clin Microbiol Rev 1992;5:248–61.
[14] van Hemert MJ, Steensma HY, van Heusden GP. 14-3-3 proteins: key regulators of cell division, signalling and apoptosis. Bioessays 2001;23:936–46.
[15] Siles-Lucas Mdel M, Gottstein B. The 14-3-3 protein: a key molecule in parasites as in other organisms. Trends Parasitol 2003;19:575–81.
[16] Gottstein B, Jacquier P, Bresson-Hadni S, Eckert J. Improved primary immunodiagnosis of alveolar echinococcosis in humans by an enzyme-linked immunosorbent assay using the Em2plus antigen. J Clin Microbiol 1993;31:373–6.
[17] Brehm K, Jensen K, Frosch P, Frosch M. Characterization of the genomic locus expressing the ERM-like protein of *Echinococcus multilocularis*. Mol Biochem Parasitol 1999;100:147–52.
[18] Louvet-Vallee S. ERM proteins: from cellular architecture to cell signaling. Biol Cell 2000;92:305–16.
[19] Felleisen R, Gottstein B. *Echinococcus multilocularis*: molecular and immunochemical characterization of diagnostic antigen II/3-10. Parasitology 1993;107(Pt 3):335–42.
[20] Matsumoto J, Muller N, Hemphill A, Oku Y, Kamiya M, Gottstein B. 14-3-3- and II/3-10-gene expression as molecular markers to address viability and growth activity of *Echinococcus multilocularis* metacestodes. Parasitology 2006;132:83–94.
[21] Halton DW. Nutritional adaptations to parasitism within the platyhelminthes. Int J Parasitol 1997;27:693–704.
[22] Siles-Lucas M, Felleisen RS, Hemphill A, Wilson W, Gottstein B. Stage-specific expression of the 14-3-3 gene in *Echinococcus multilocularis*. Mol Biochem Parasitol 1998;91:281–93.
[23] Siles-Lucas M, Merli M, Gottstein B. 14-3-3 proteins in *Echinococcus*: their role and potential as protective antigens. Exp Parasitol 2008;119:516–23.
[24] Rosas G, Fragoso G, Garate T, Hernández B, Ferrero P, Foster-Cuevas M, et al. Protective immunity against *Taenia crassiceps* murine cysticercosis induced by DNA vaccination with a *Taenia saginata* tegument antigen. Microbes Infect 2002;4:1417–26.

ARTICLE IN PRESS
PARINT-00817; No of Pages 9
Parasitology International xxx (2010) xxx–xxx
Contents lists available at ScienceDirect
Parasitology International
journal homepage: www.elsevier.com/locate/parint

Transcripts analysis of infective larvae of an intestinal nematode, *Strongyloides venezuelensis*

Ayako Yoshida [a], Eiji Nagayasu [a], Anna Nishimaki [a], Akira Sawaguchi [b], Sayaka Yanagawa [a], Haruhiko Maruyama [a,*]

[a] Department of Infectious Diseases, Division of Parasitology, Faculty of Medicine, University of Miyazaki, Miyazaki, Japan
[b] Department of Anatomy, Division of Ultrastructural Cell Biology, Faculty of Medicine, University of Miyazaki, Miyazaki, Japan

ARTICLE INFO

Article history:
Received 14 April 2010
Received in revised form 4 October 2010
Accepted 27 October 2010
Available online xxxx

Keywords:
Strongyloides
Nematode
Infective larva
EST

ABSTRACT

Free-living infective larvae of *Strongyloides* nematodes fulfill a number of requirements for the successful infection. They need to endure a long wait in harsh environmental conditions, like temperature, salinity, and pH, which might change drastically from time to time. Infective larvae also have to deal with pathogens and potentially hazardous free-living microbes in the environment. In addition, infective larvae must recognize the adequate host properly, and start skin penetration as quickly as possible. All these tasks are essentially important for the survival of *Strongyloides* nematodes, however, our knowledge is extremely limited in any one of these aspects. In order to understand how *Strongyloides* infective larvae meet these requirements, we examined transcripts of infective larvae by randomly sequencing cDNA clones constructed from *S. venezuelensis* infective larvae. After assembling successfully sequenced clones, we obtained 162 unique singletons and contigs, of which 84 had been significantly annotated. Annotated genes included those for respiratory enzymes, heat-shock proteins, neuromuscular proteins, proteases, and immunodominant antigens. Genes for lipase, small heat-shock protein, globin-like protein and cytochrome *c* oxidase were most abundantly transcribed, though genes of unknown functions were also abundantly transcribed. There were no hits found against NCBI or NEMABASE4 for 37 (22.3%) EST out of the total 162 EST. Although most of the transcripts were not infective larva-specific, the expression of respiration related proteins was most actively transcribed in the infective larva stage. The expression of astacin-like metalloprotease, small heat-shock protein, *S. stercoralis* L3Nie antigen homologue, and one unannotated and 2 novel genes was highly specific for the infective larva stage.

1. Introduction

Strongyloidiasis is endemic in tropical and subtropical regions, such as Southeast Asia, Latin-America, and sub-Saharan Africa, and endemic foci are present in temperate countries as well, e.g. Mediterranean coast of Spain, southern United States, and Satsunann-Ryukyu Islands in Japan [1–3]. Hundreds of millions of people have been possibly affected globally, though no precise estimate is available.

The key for the control of strongyloidiasis is in the infective larva because the infection starts with this stage of the worm. Free-living infective larvae develop from eggs deposited by free-living females in the soil or parasitic females in the infected host. Infective larvae then wait a host to be infected for some time in the external environment. Considering the life of infective larvae, they obviously face a number of hard tasks before they finally find the host.

First, they are required to endure physical and chemical conditions among them. Temperature, salinity, and pH might change drastically during the wait and chemical compounds could contaminate their surroundings. Second, they have to get rid of or get along with pathogens and potentially hazardous free-living microbes. Among them are various kinds of viruses, bacteria, parasites, and fungi. Infective larvae should be equipped with a kind of defense mechanisms as free-living nematodes are [4,5]. Otherwise they would be heavily infected before they infect the host. In addition to the protection against a number of environmental factors, they must recognize appropriate host animals and start skin penetration as quickly as possible. Failure in host-finding and infection processes would result in the extinction of the species.

Strongyloides infective larvae definitely have solutions to all of the problems and situations described above, however, little is known about their survival and infection strategies [6]. It would be of great scientific and practical significance to understand the biological processes taking place in *Strongyloides* infective larvae. For example, because infection control cannot be done solely with a mass treatment of humans and animals due to the adverse side effects of drugs on biological diversity, new strategies to control the infection have to be explored based on the biology of the nematodes [7,8].

* Corresponding author. 5200 Kihara, Kiyotake, Miyazaki 889-1692, Japan. Tel.: +81 985 85 0990; fax: +81 985 84 3887.
E-mail address: hikomaru@med.miyazaki-u.ac.jp (H. Maruyama).

1383-5769/$ – see front matter © 2010 Elsevier Ireland Ltd. All rights reserved.
doi:10.1016/j.parint.2010.10.007

Please cite this article as: Yoshida A, et al. Transcripts analysis of infective larvae of an intestinal nematode, *Strongyloides venezuelensis*, Parasitol Int (2010), doi:10.1016/j.parint.2010.10.007